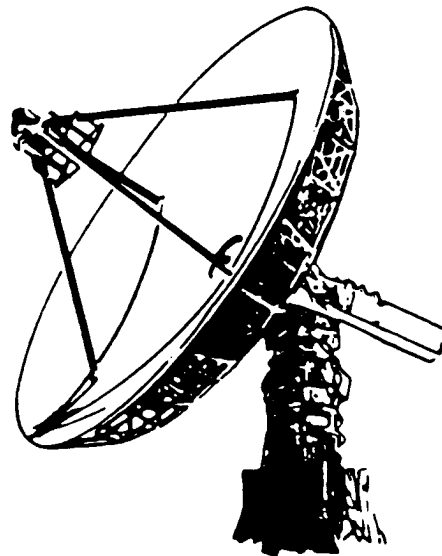


DETERMINING THE MEASUREMENT ACCURACY OF THE HP 8510 MICROWAVE NETWORK ANALYZER

Bruce Donecker
Network Measurements Division
1400 Fountain Grove Parkway
Santa Rosa, California 95401

**RF & Microwave
Measurement
Symposium
and
Exhibition**

 **HEWLETT
PACKARD**



System Performance Dimensions

Parameter (S11, S21, S12, S22)

Test Set

Connector Type and Sex

Calibration Standards

Calibration Method

Actual Device Parameters

Test Port Cables

Source (Frequency Accuracy)

Sweep Mode

Sweep Speed

Power Level

Environmental Conditions

Averaging

Smoothing

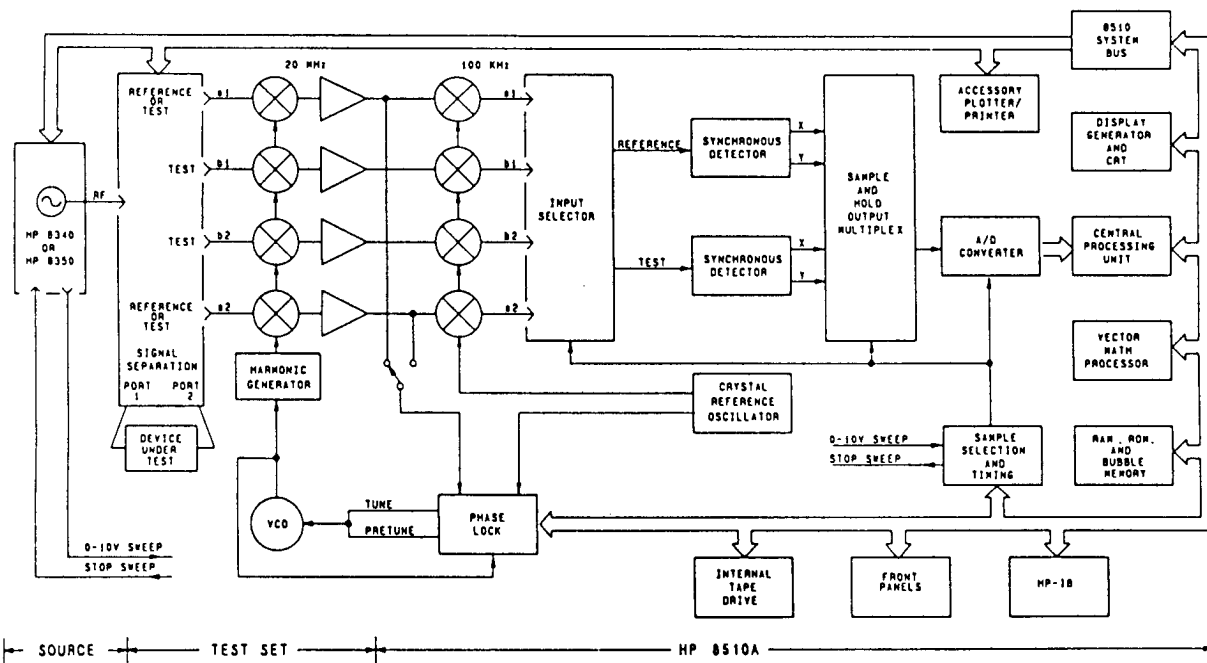
Gating

System Performance Dimensions

In addition to the performance of the individual instruments, it is found that overall measurement accuracy depends strongly upon system configuration and user-selected operating conditions. The most significant factors are listed in the table.

If an accuracy specification were written for each possible system configuration and measurement condition, several thousand specifications would need to be generated and supported. Although this approach is impractical to manage, the user still requires the ability to characterize system performance for an arbitrary configuration and set of measurement conditions.

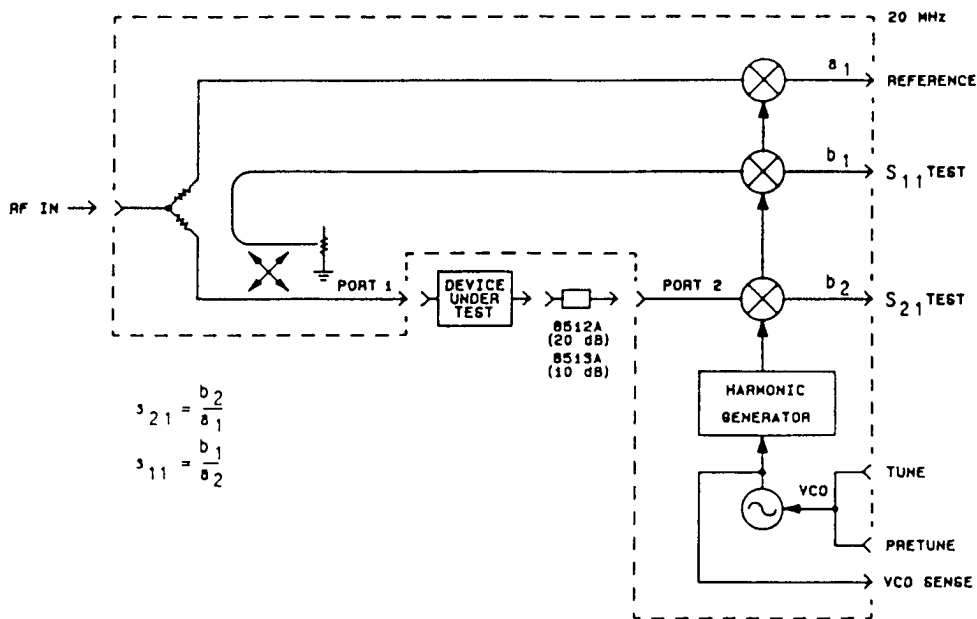
8510 Simplified System Block Diagram



Overall simplified Block Diagram

Potential instrumentation errors exist in the Following locations:

1. Source frequency (absolute and drift errors)
2. Signal crosstalk between channels through the L.O. ports
3. Gain errors in the input selectors (each output channel contains four stages of auto-ranging I.F. amplification)
4. D.C. offset in the output stages of the synchronous detectors
5. Non-unity gain ratio between the X and Y axes of the detectors
6. Quadrature error between the X and Y axes of the detectors
7. Non-linearity of the A/D converter
8. Overall noise floor of the signal path
9. Overall compression characteristic of the signal path
10. I.F. residual signals due to L.O. leakage into the signal paths
11. Effects of phase noise from the signal and L.O. carriers



Reflection/Transmission Test Sets Signal Flow.

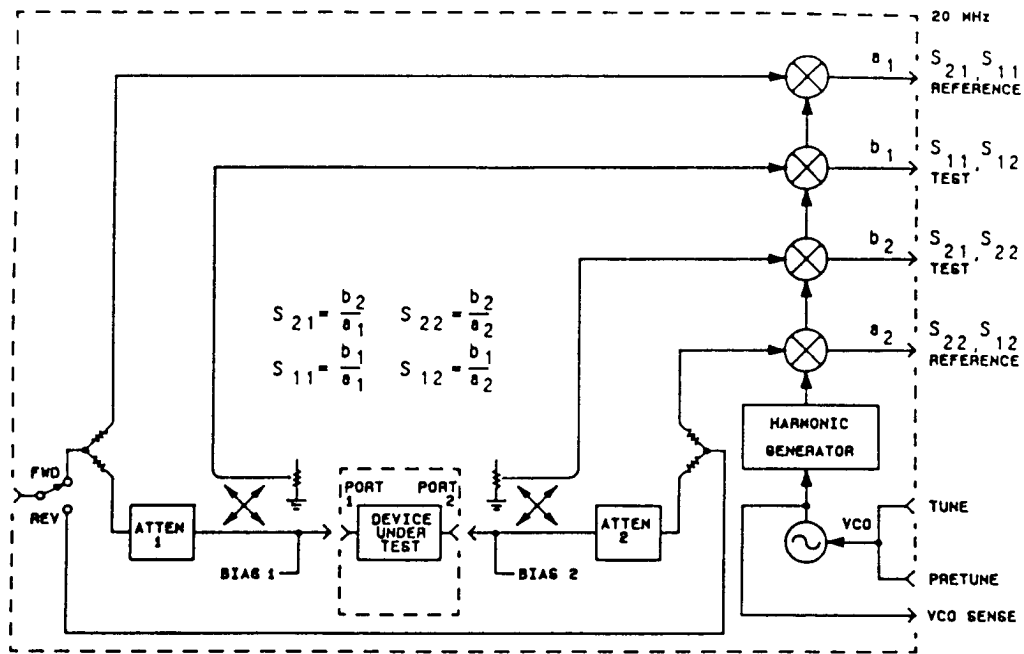
Reflection/Transmission Test Set Block Diagram

This simplified block diagram shows the main signal path components of the HP 8512A and 8513A Test Sets. The reference path is electrically balanced to provide a nominal magnitude and phase match of the reflection and transmission paths. Directivity is determined by the directional coupler (8512A) or bridge (8513A). In the case of the 8512A, source match is determined by the port match of the power splitter by the match of the main line of the coupler. In the case of the 8513A, source match is determined primarily by the bridge, since the match of the splitter is buffered by the insertion loss (6 dB) of the main signal path of the bridge. The match of the return port is determined primarily by the external pad rather than the match the Port 2 sampler.

The VCO drives a fast pulse generator to provide the local oscillator signal. Harmonics of the L.O. mix in the samplers with the microwave test signals to produce a 20 MHz first I.F. The reference channel I.F. feeds the phase-lock system to control the L.O. frequency.

Potential instrumentation errors exist in the following locations:

1. Signal crosstalk between channels through the L.O. ports
2. Frequency response tracking errors between the individual sampling frequency converter channels
3. High level compression in the sampling frequency converter
4. Broad-band noise floor of the sampling frequency converter
5. Frequency response of the coupled arm of the directional coupler
6. Finite directivity of the directional coupler
7. Source and load match at the test ports of the test set



S-Parameter Test Sets Signal Flow.

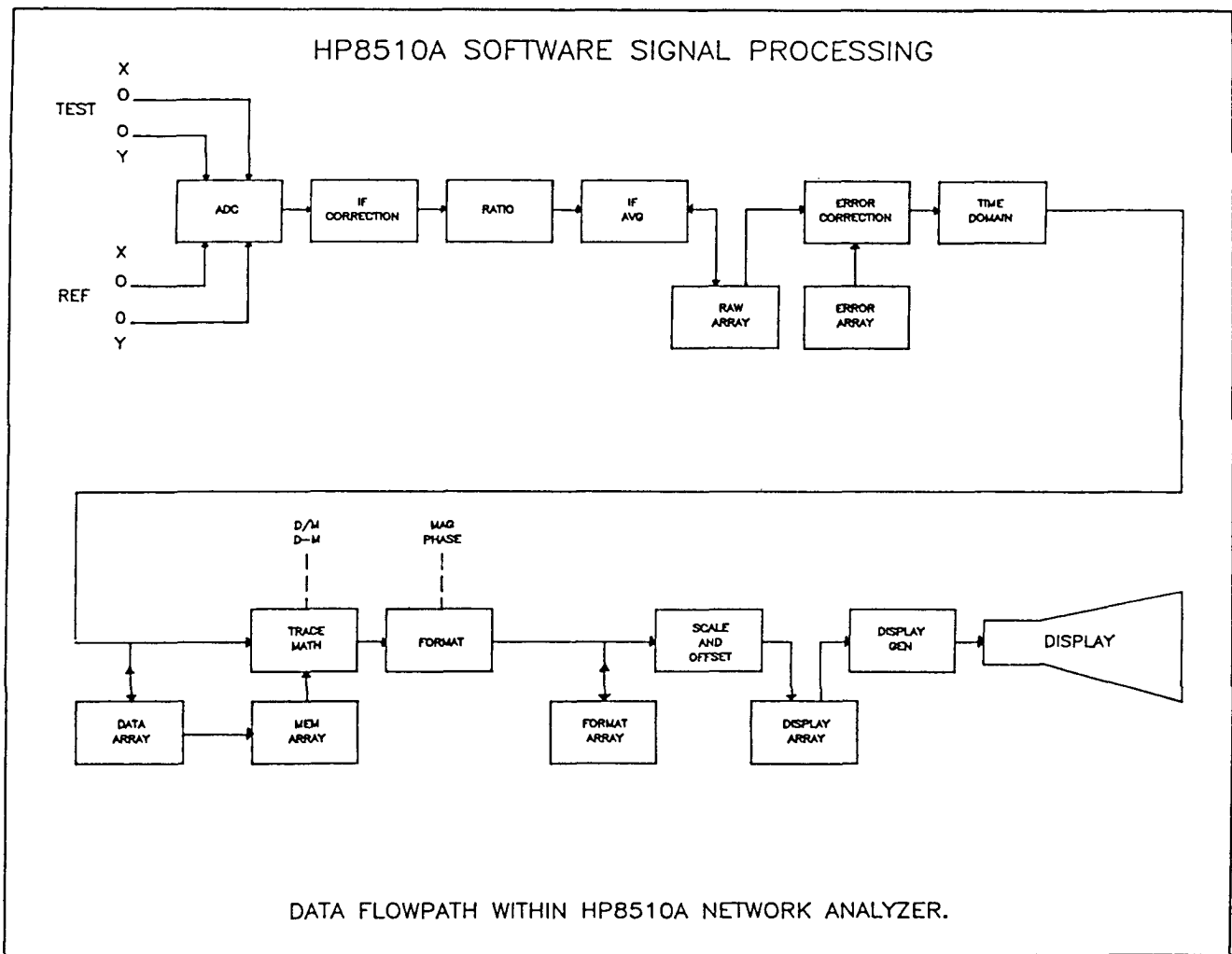
S-Parameter Test Set Block Diagram

The S-Parameter test sets, the coupler-based HP 8514A and the bridge-based 8515A, build on the concepts of the 8512A and 8513A adding a variety of notable capabilities: fast electronic transfer switching, step attenuators, and bias tees. Note that the transfer switch is located prior to the ratio nodes, thus ensuring a high degree of repeatability. Additionally, the use of a fourth sampler channel avoids the need to utilize microwave switches in the test channels, again greatly enhancing repeatability.

Directivity characteristics are very similar to the reflection/transmission test sets. The port matches of the 8514 are influenced by the bias tee and step attenuator in addition to the items noted for the 8512. The port matches of the 8515 are very similar to Port 1 of the 8513.

Potential instrumentation errors exist in the following locations:

1. Signal crosstalk between channels through the L.O. ports
2. Frequency response tracking errors between the individual sampling frequency converter channels
3. High level compression in the sampling frequency converter
4. Broad-band noise floor of the sampling frequency converter
5. Frequency response of the coupled arm of the directional coupler
6. Finite directivity of the directional coupler
7. Source and load match at the test ports of the test set
8. Signal crosstalk through the "off" path of the transfer switch
9. Attenuator repeatability (if switched)

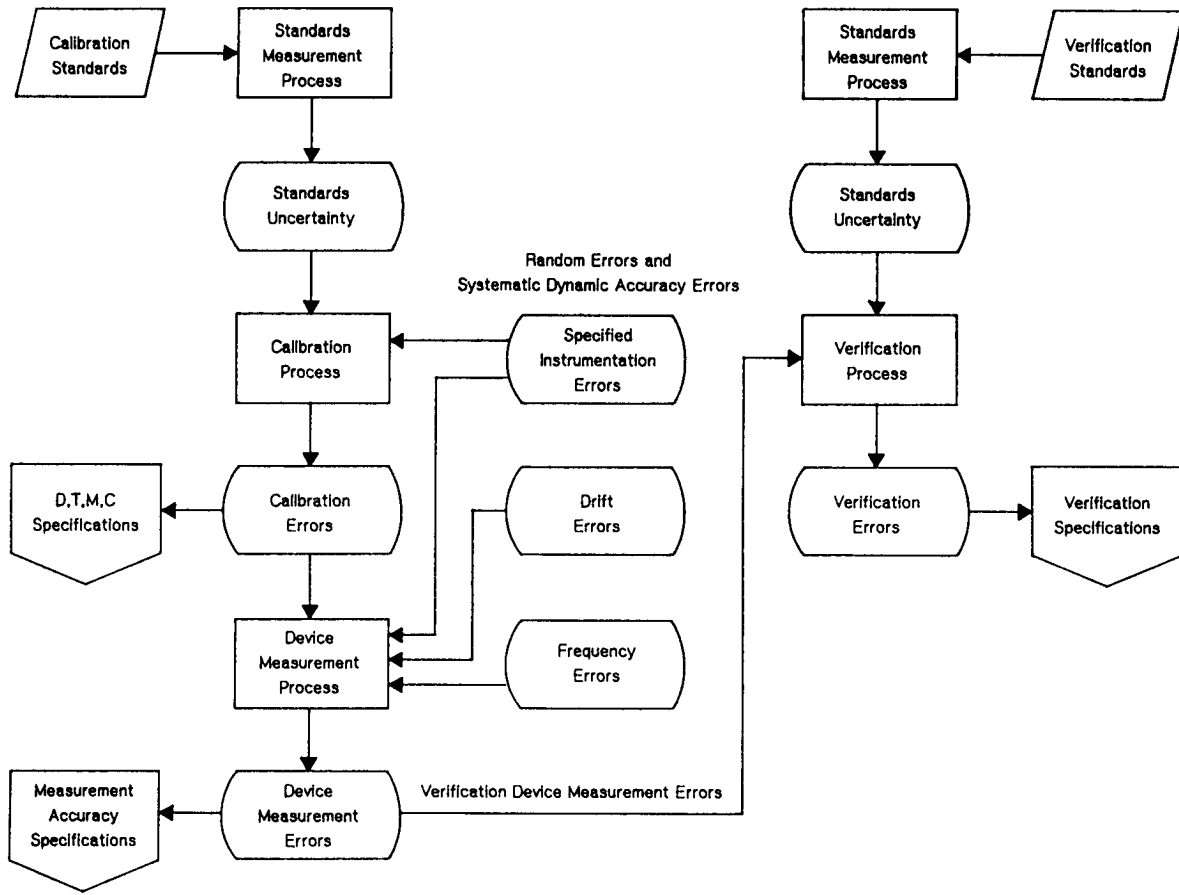


8510 Software Signal Processing / Data Flowpath

Assuming proper characterization of the calibration standards, computation errors are limited primarily to roundoff/truncation errors throughout the processing chain. Typical degradation is less than two bits out of sixteen.

The error correction block enhances measurement accuracy as a result of the microwave calibration process. The I.F. correction block enhances measurement accuracy as a result of periodic calibration of the 100 KHz I.F. system (autoranging gain, D.C. offset, differential gain of the X and Y axes, quadrature of the X and Y axes, ADC linearity).

Specification Generation Flowgraph



Specification Generation Flowgraph

The basis for a reliable system specification is a traceable path to fundamental standards and sound theoretical principles. As shown in the flowgraph, the standards carry uncertainties from the process used to measure their properties. Hopefully these errors are small compared with expected system errors.

The system model assumes that a similarly detailed method has been used to generate the individual instrument specifications. The instrumentation errors combine with the standards uncertainties in a manner determined by the calibration process and result in a set of specifications for the calibration residuals (effective directivity, tracking, match, and crosstalk). Now D, T, M, and C may be combined with the instrumentation errors in the device measurement process to produce a measurement accuracy specification.

The verification process involves the measurement of an independent set of precision devices. Therefore, the verification specifications must include the combined errors of the device measurement process and the verification standards measurement.

Types of Error Sources

- Systematic
- Random
- Drift

Types of Error Sources

Systematic errors result from the stable imperfections and inaccuracies associated with the standards and instrument hardware. The manner in which systematic errors combine is affected by the calibration and measurement methods and the degree of computational precision.

Random errors result from the normal variations which are characteristic of a given process. In the present case, only those items which have a zero mean value are included. Items which have a non-zero mean are included with the systematic errors where variations about the mean may be characterized.

Drift errors are considered to be time or temperature dependent performance characteristics.

Systematic Error Sources

- D = Directivity
- Ms = Source Match
- Tr = Reflection Tracking

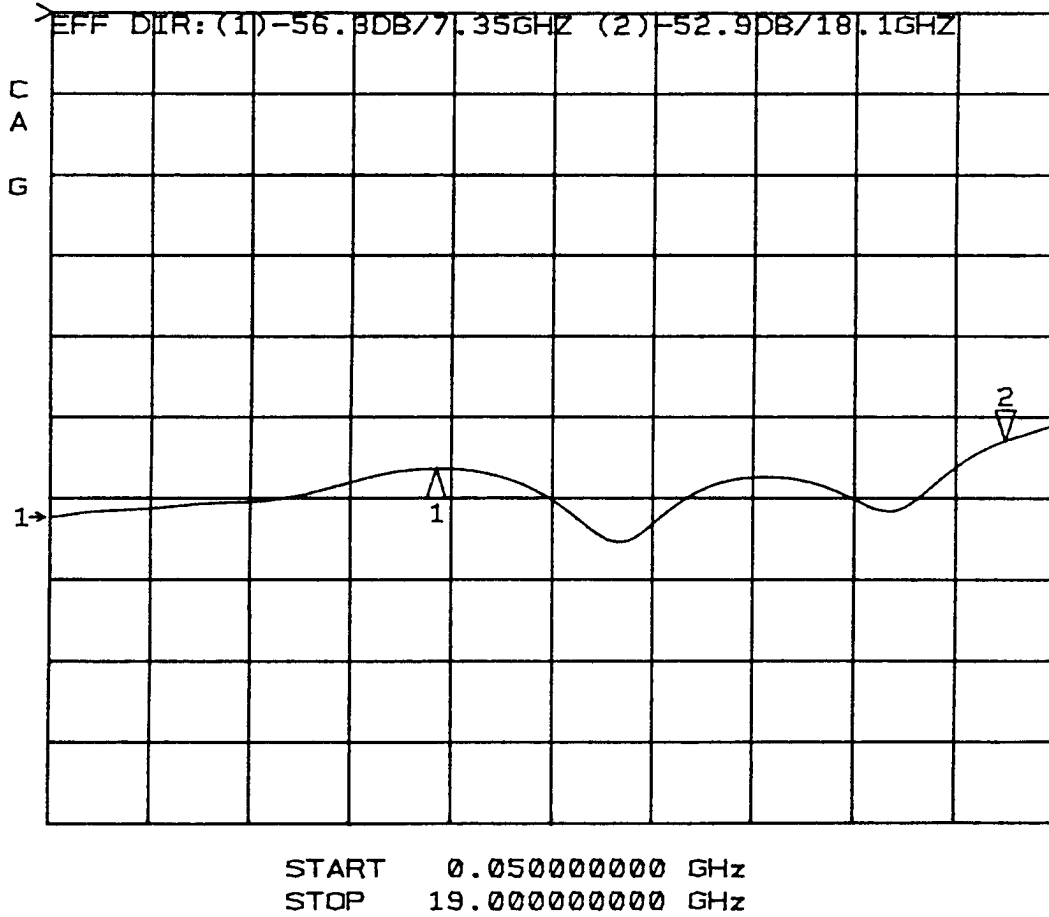
- C = Crosstalk
- Ml = Load Match
- Tt = Transmission Tracking
- Cs = Cable Stability (Deg./GHz)

- A = Dynamic Accuracy
- F = Frequency

Systematic Error Sources

Residual (post-calibration) errors result from the imperfections in the calibration standards, the connector interface, the interconnecting cables and the instrumentation. All measurements are affected by Dynamic Accuracy and Frequency error effects. For reflection measurements, the associated residual errors are: Effective Directivity, Effective Source Match, and Effective Reflection Tracking. For transmission measurements, the additional residual errors are: Effective Crosstalk, Effective Load Match, Effective Transmission Tracking, and Cable Stability.

S11 log MAG
 REF 0.0 dB
 10.0 dB/

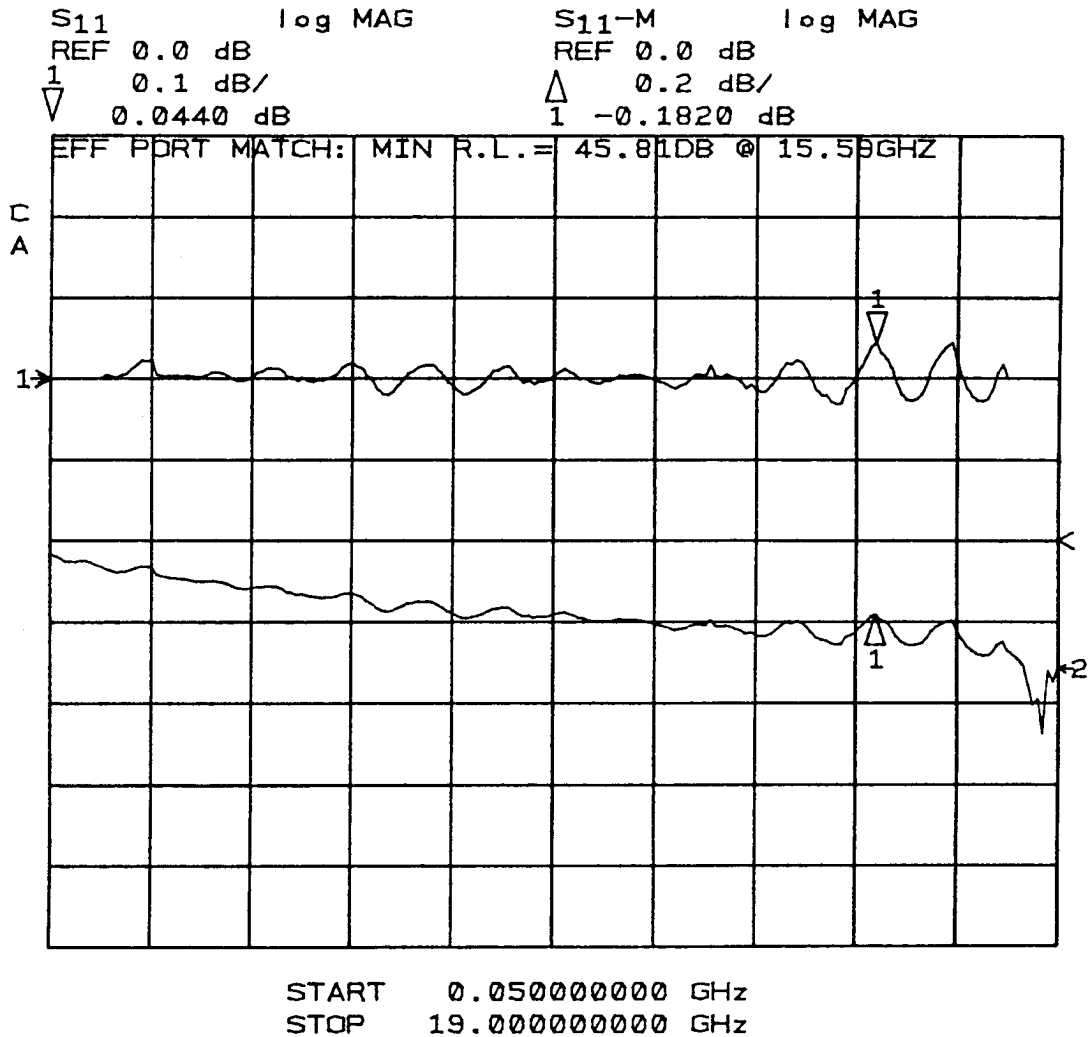


D - Effective Directivity Plot

This is a post-calibration S11 measurement of a 30 cm. beadless airline cascaded with a fixed termination; the airline is a precision factory-level standard. The measurement utilizes the Time Domain feature to remove the effects of the fixed termination by Gating. The result of this measurement is a comparison of the calibration to a precision reference 50 Ohm transmission line, thus extracting the Effective Directivity.

The primary error sources are: center conductor positioning, slide stability, and Zo of the calibration load.

This plot is typical of performance normally achieved in 7 mm. Note the worst case value of -52.9 dB at 18 GHz; the specification is -50 dB (.5 - 18 GHz).



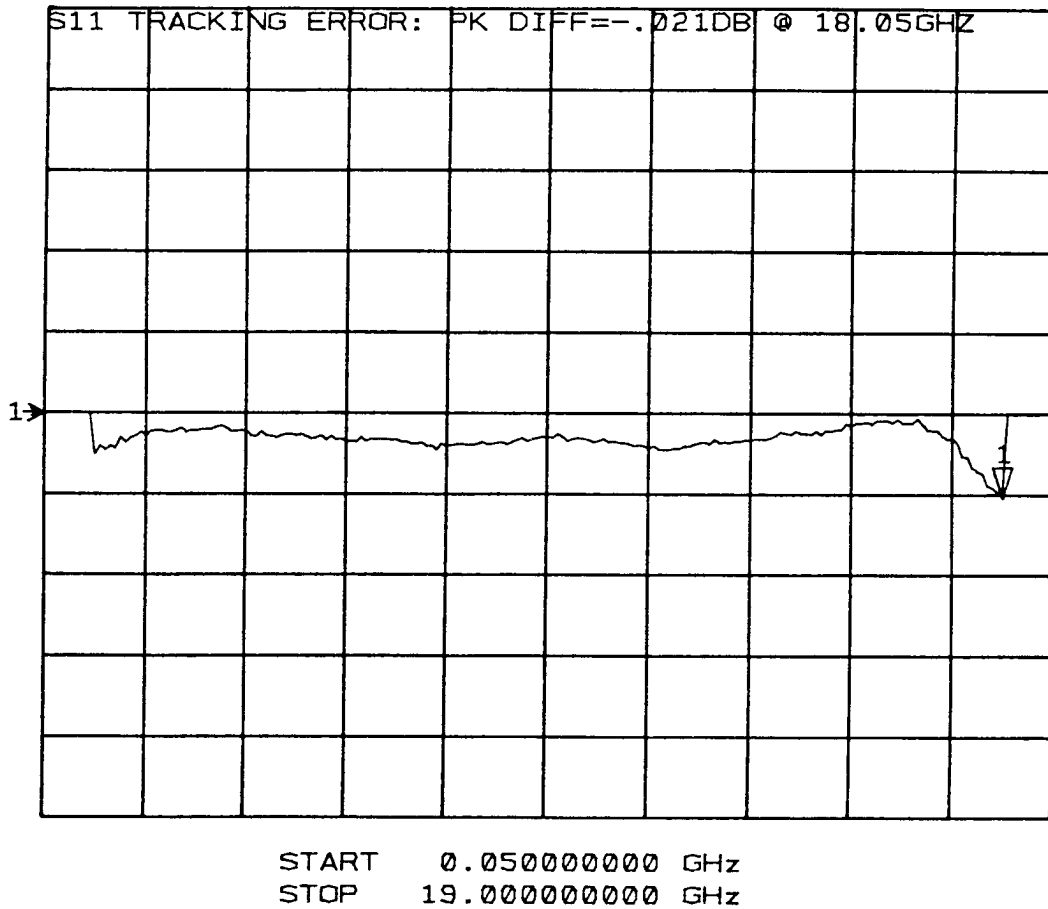
Ms - Effective Source Match Plot

The lower trace is an S11 measurement of the precision airline cascaded with a 7 mm planar short. The upper trace is the same measurement after the effects of loss and Effective Directivity have been removed; this results in a display of the interaction between the short and the Effective Source Match. Now the Effective Source Match may be calculated from the magnitude of the ripple; the ripple period is a result of airline length.

The primary error source is the capacity model of the shielded open. A secondary source of error is the sliding load.

This plot is typical of performance normally achieved in 7 mm. Note the worst case value of -45.8 dB at 15.5 GHz; the specification is -40 dB (.5 - 18 GHz).

S11 log MAG
REF 0.0 dB
0.02 dB/

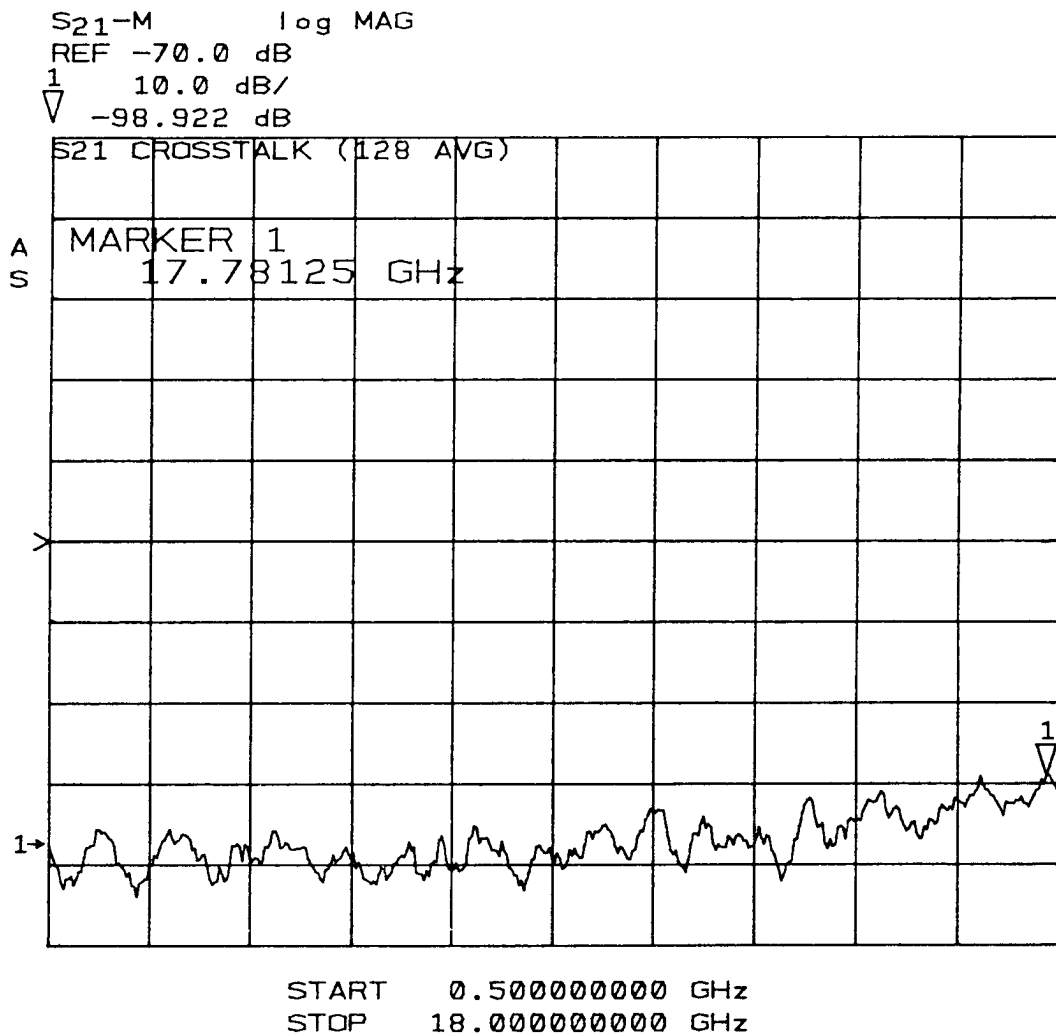


Tr - Effective Reflection Tracking Plot

This plot results from an S11 measurement of the precision airline cascaded with a 7 mm planar short after the effects of loss, Effective Directivity, and Effective Source Match have been removed.

The primary error source is the capacity model of the shielded open.

This plot is typical of performance normally achieved in 7 mm. Note the worst case value of .021 dB at 18 GHz; the specification is +/- .05 dB (.5 - 18 GHz).

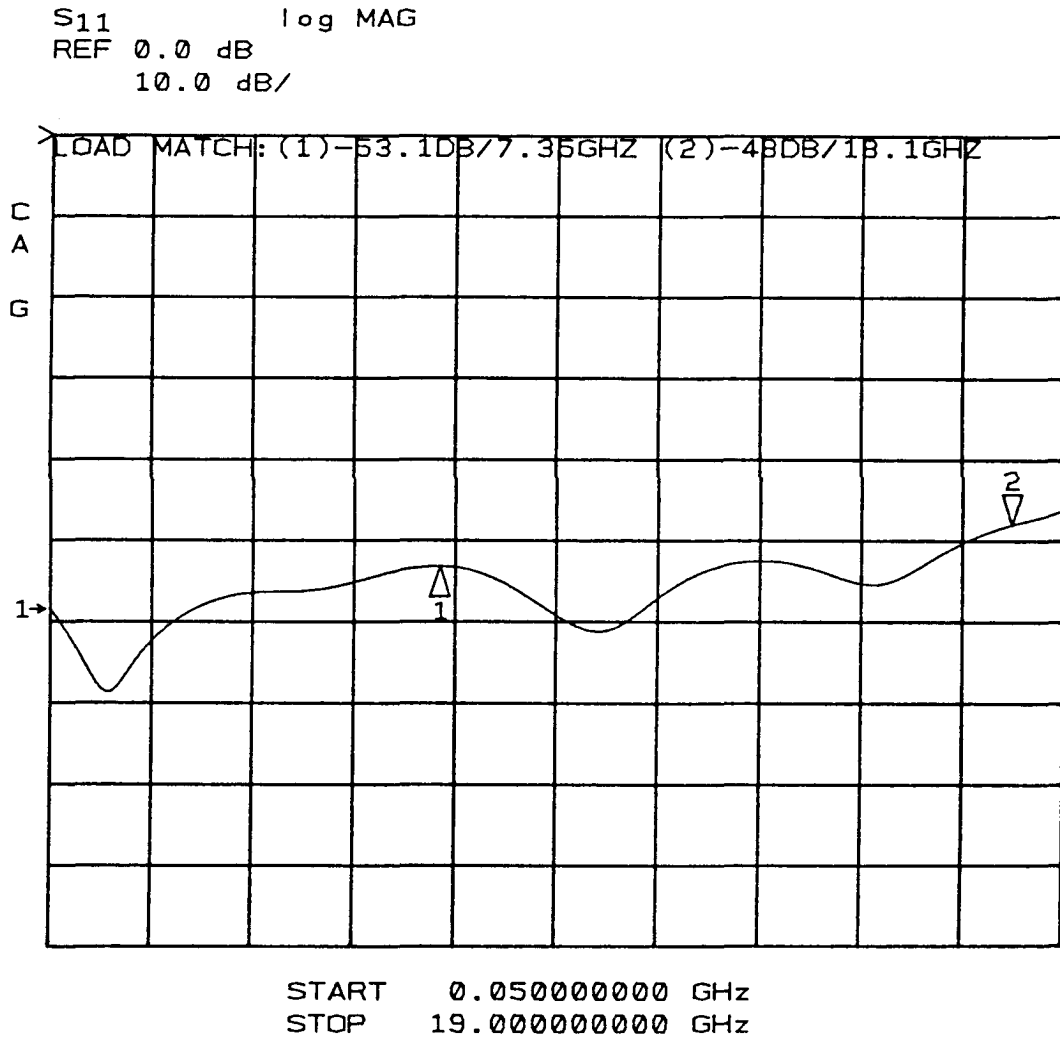


C - Effective Crosstalk Plot

This plot is a measurement of transmission residuals after the manual system crosstalk has been characterized and removed as a part of the vector error correction process. It is referenced to a through connection in the normal transmission measurement configuration.

Primary error sources are I.F. residuals and noise while quantizing characteristics play a secondary role.

This plot is typical of performance normally achieved in 7 mm. Note the worst case value of -98.9 dB at 17.7 GHz; the specification is -90 dB (.5 - 18 GHz).



MI - Effective Load Match Plot

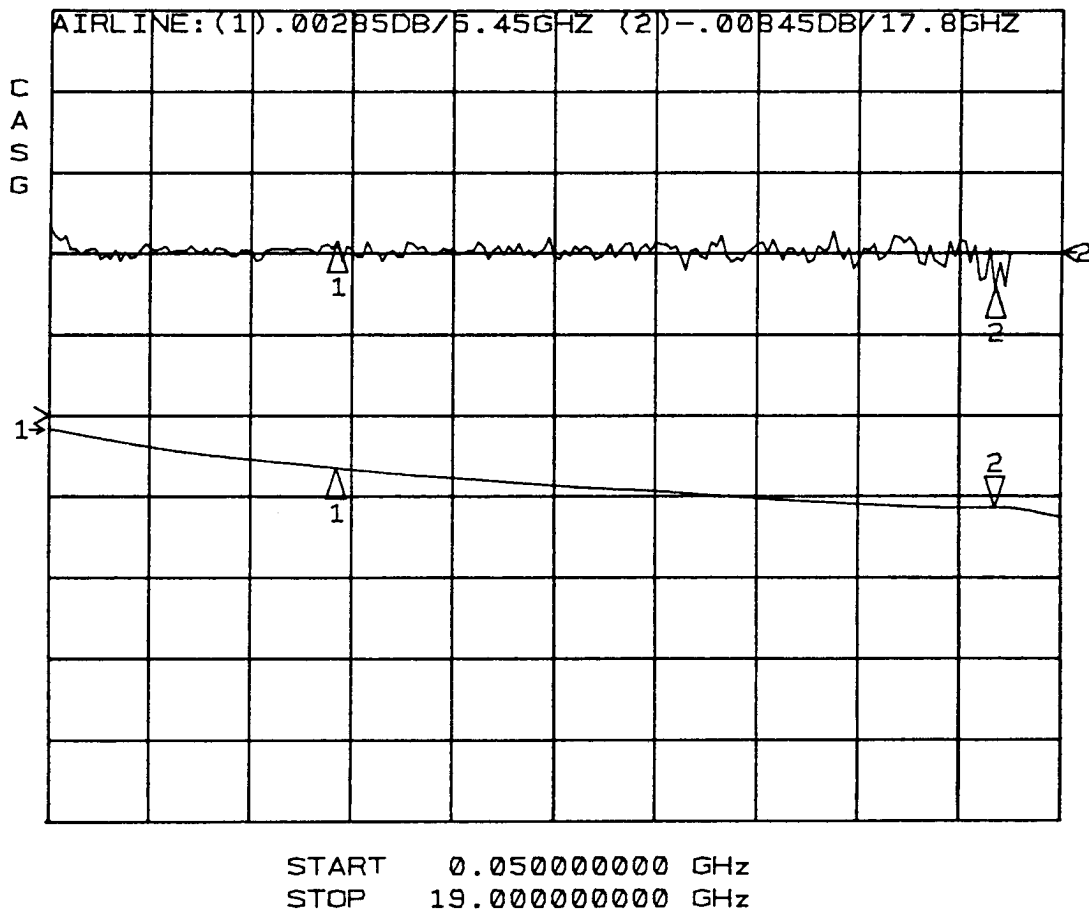
This plot shows an S11 measurement of the load port of the test set. It has been measured with the reflectometer of the source port and the effects of Effective Directivity and Source Match have been removed. Like several other measurements, this one is referenced to a precision airline (factory-level standard).

Primary error sources are the sliding load and connector repeatability.

This plot is typical of performance normally achieved in 7 mm. Note the worst case value of -48 dB at 18 GHz; the specification is -40 dB (.5 - 18 GHz).

S21 log MAG
 REF 0.0 dB
 0.1 dB/

S21 log MAG
 REF 0.0 dB
 0.02 dB/



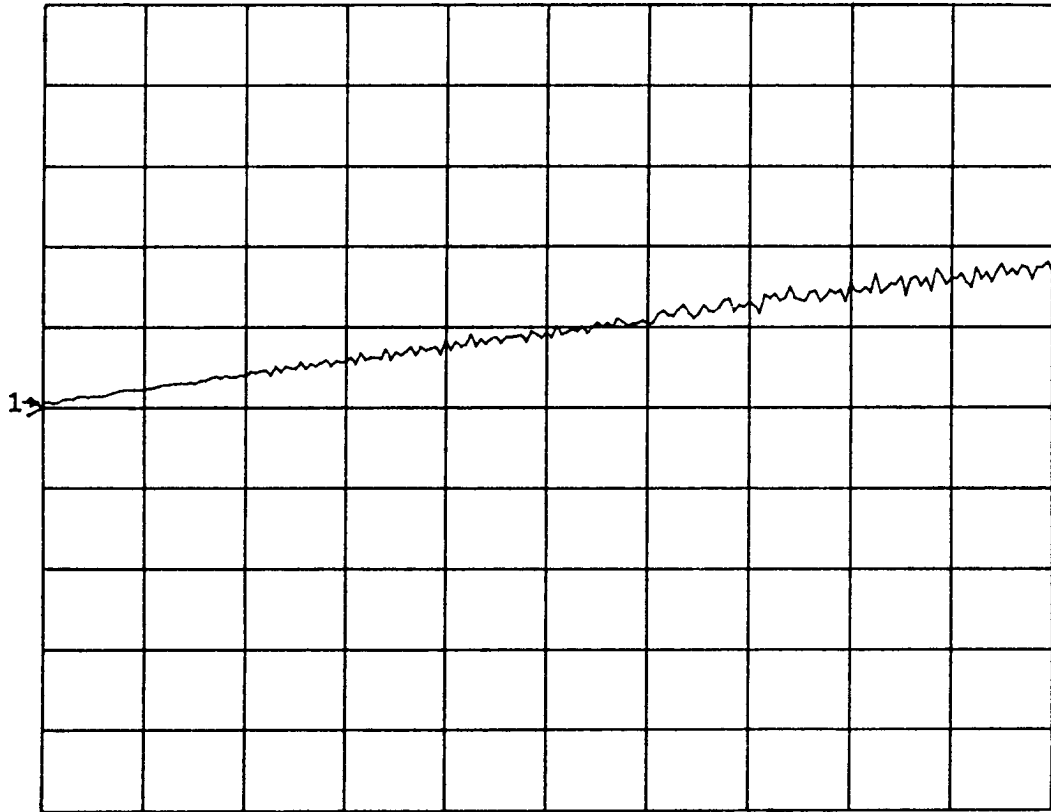
Tt - Effective Transmission Tracking Plot

The lower trace is a smoothed (5% moving average) S21 measurement of the precision airline; the droop is caused by loss. The upper trace is the difference between a smoothed and a non-smoothed S21 measurement. The smoothed measurement filters the vector interaction between the source and load matches, while the non-smoothed measurement does not. Effective Transmission Tracking is the result of this interaction (ripple).

The primary sources of error are the uncorrected Load Match and the Effective Source Match.

This plot is typical of performance normally achieved in 7 mm. Note the worst case value of .008 dB at 17.8 GHz; the specification is +/- .015 dB (.5 - 8 GHz); +/- .030 dB (8 - 18 GHz).

S11/M ∠
REF 0.0 °
500.0 m°/



START 0.500000000 GHz
STOP 18.000000000 GHz

Cs - Cable Phase Stability Plot - S21 Phase

This plot shows the change in phase which results when a test port extension cable is bent from a straight condition into a 180 degree curve around a 6 inch diameter mandrel. Only phase is shown, since the amplitude stability is very good and rarely a source of concern.

The primary source of error is the physical bending characteristic of the cable.

This plot is typical of performance normally achieved in 7 mm. Note the worst case value of .9 deg. at 18 GHz; the specification is .1 deg./GHz.

Dynamic Accuracy Error (A)

- E_a = I.F. Autorange Gain Error
- E_{co} = Compression Error
- E_{ci} = Circularity Error
- E_{dc} = Effective D.C. Offset Error
- E_l = I.F. Linearity Error
- E_r = I.F. Residual Signal Error

- G_a = I.F. Autorange Gain
- G_s = Sampler Gain

A - Dynamic Accuracy Error Components

E_a results from characterization errors during self-calibration.
(+/- .005 dB max for stages 1, 2; +/- .010 dB max for stages 3, 4)

E_{co} is caused primarily by gain compression in the microwave frequency converter (sampler) at high signal levels.
(.1 dB max at -10 dBm)

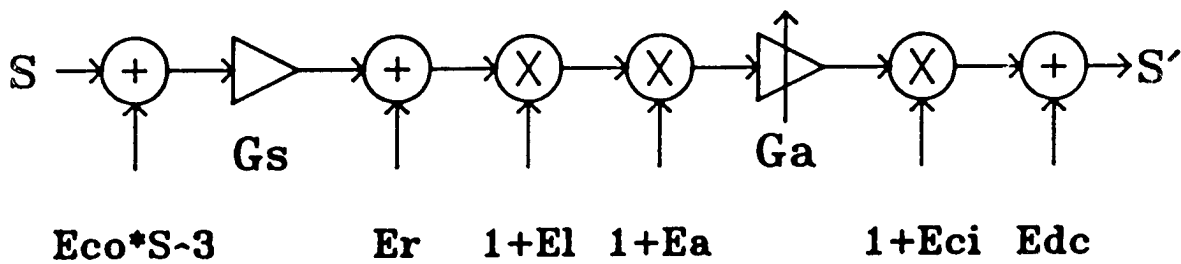
E_{ci} and E_{dc} errors are generated in the synchronous detectors.
(+/- .003 dB max and -100 dBm max)

E_l results from localized non-linearities in the I.F. filter system.
(+/- .003 dB max)

E_r results from L.O. leakage into the I.F. signal paths.
(-120 dBm max)

8510 Dynamic Accuracy Model

The following model is used to construct the dynamic accuracy curves for the various configurations of the 8510 system. These curves are plotted in Section 1-1 of the 8510 Operating and Service Manual.



E_a = I.F. autorange gain error

E_{co} = compression error

E_{ci} = circularity Error

E_{dc} = effective D.C. offset error

E_l = I.F. linearity error

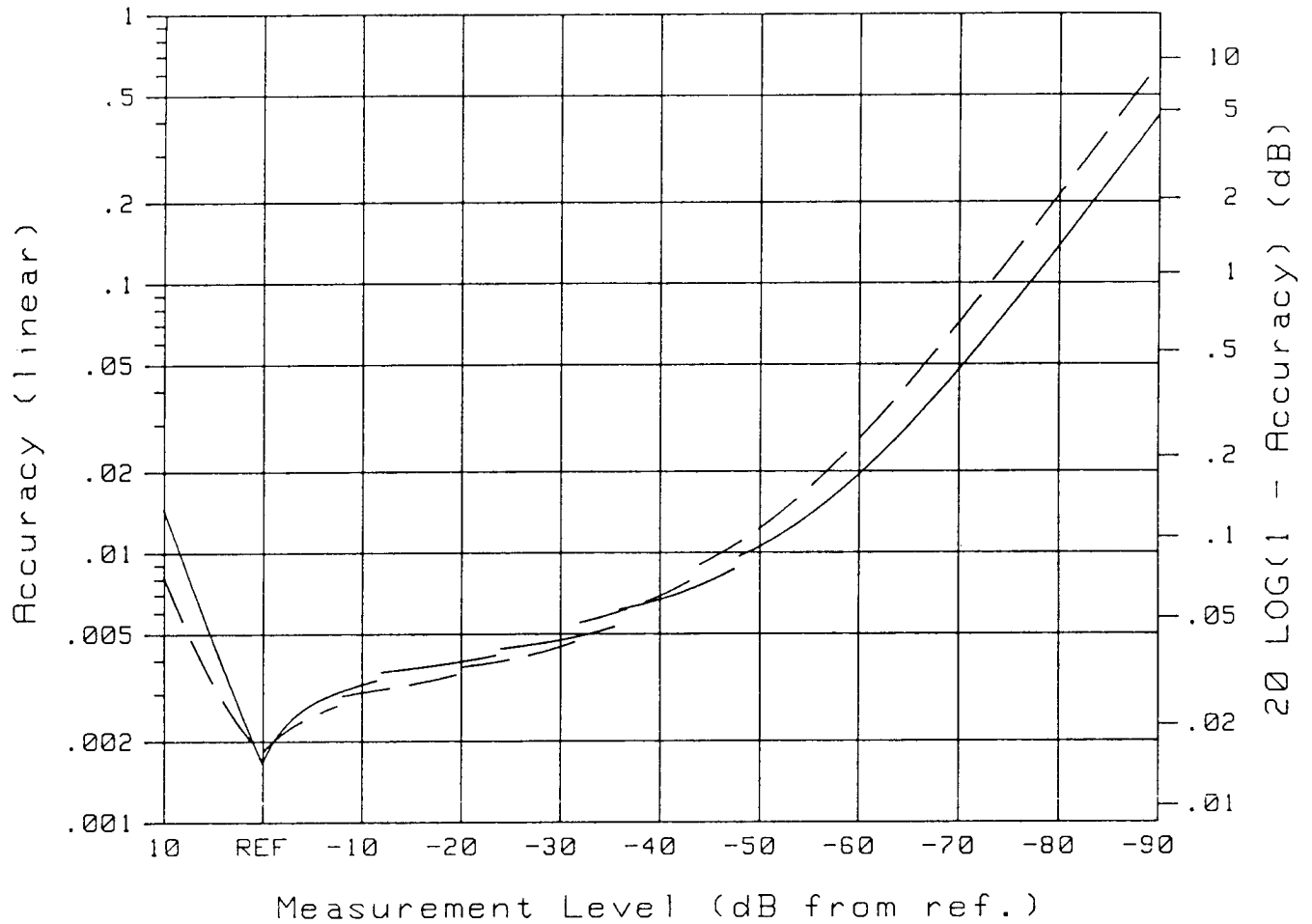
E_r = I.F. residual signal error

G_a = I.F. autorange gain

G_s = sampler gain

where all the terms are expressed in linear format.

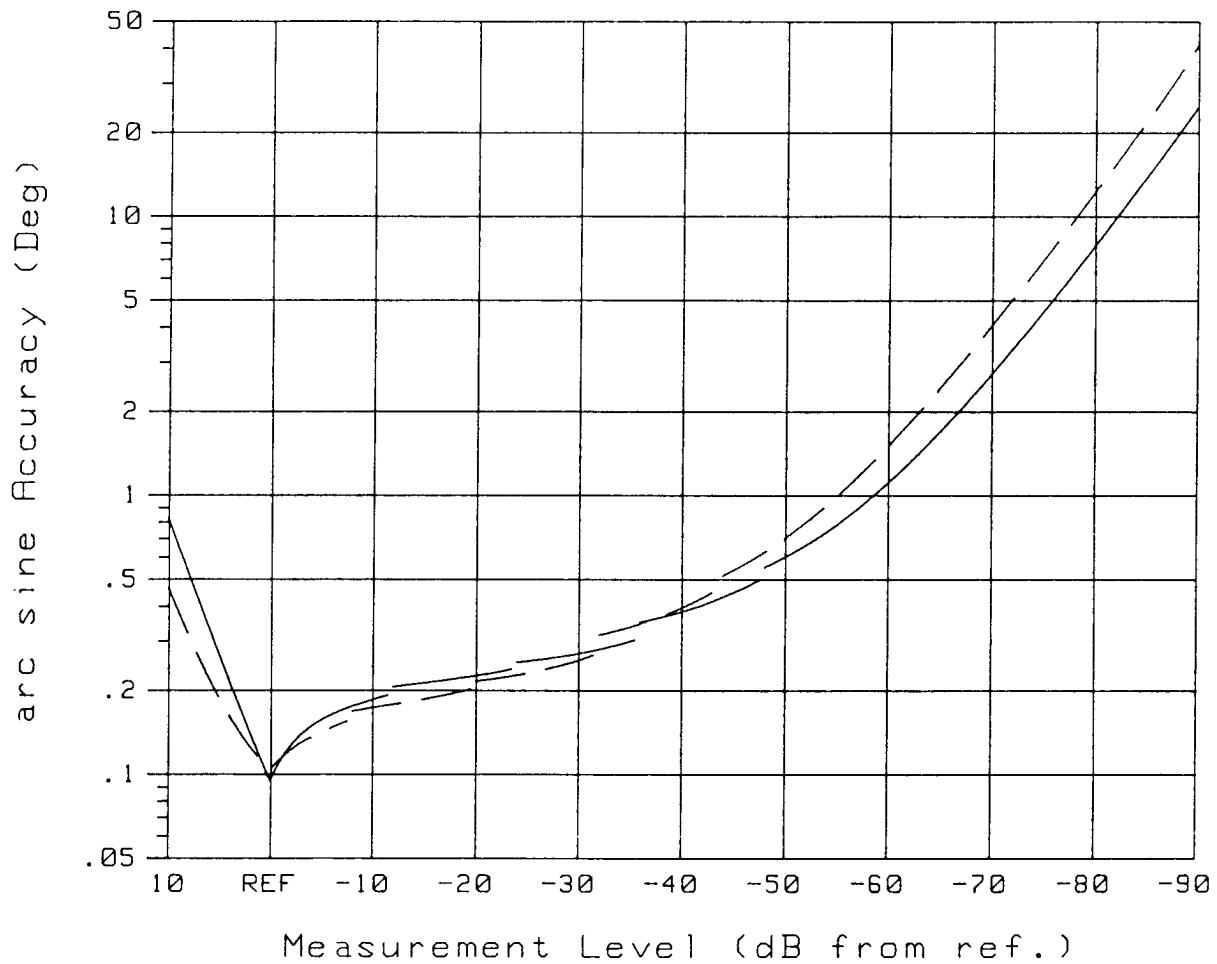
Am = Dynamic Accuracy, Magnitude Uncertainty



Am - Dynamic Accuracy Magnitude Plot

This plot shows overall magnitude detection accuracy as a function of level for signals of arbitrary phase. It assumes a system calibration at the predefined REF level. The solid-line curve represents a worst case performance limit at 8 GHz, while the dashed-line curve is the limit at 18 GHz.

Ap = Dynamic Accuracy, Phase Uncertainty



Ap - Dynamic Accuracy Phase Plot

This plot shows overall phase detection accuracy as a function of level for signals of arbitrary phase. It assumes a system calibration at the predefined REF level. The solid-line Curve represents a worst case performance limit at 8 GHz, while the dashed-line curve is the limit at 18 GHz. Phase uncertainty is calculated on a worst-case basis from the magnitude uncertainty and the signal level; $A_p = \text{Arcsin} (A_m / \text{signal level})$.

Random Error Sources

- N_h = High Level Noise (rms)
- N_l = Low Level Noise (rms)

- R_{r1} = Port 1 Reflection
Repeatability Error
- R_{t1} = Port 1 Transmission
Repeatability Error
- R_{r2} = Port 2 Reflection
Repeatability Error
- R_{t2} = Port 2 Transmission
Repeatability Error

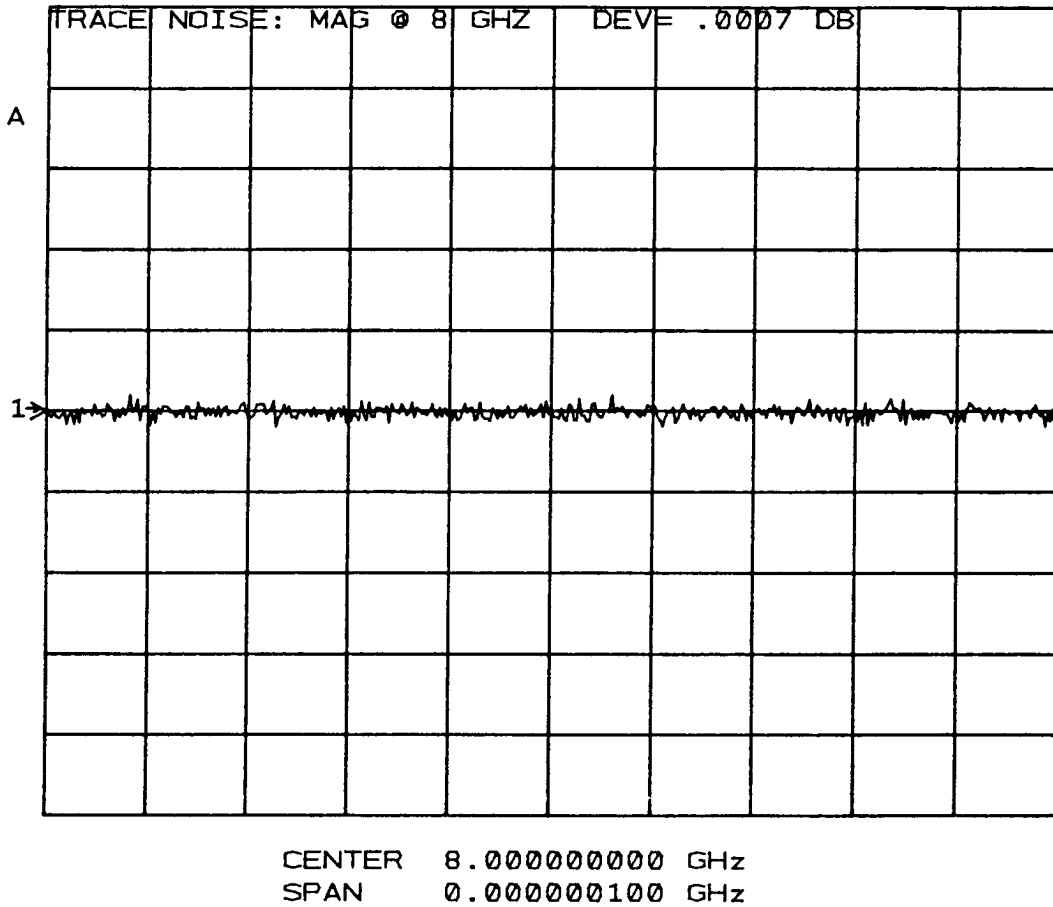
Random Error Sources

N_h is caused by phase noise on the microwave signal source and the local oscillator. The effect is to cause noise or jitter on the measurement trace even when signal levels are high. It results from a spectral bandwidth which exceeds the detection bandwidth.

N_l is set by the broadband noise floor of the entire receiver.

R_{r1} , R_{t1} , R_{r2} , and R_{t2} are all caused by the random variations encountered in connecting a pair of 7 mm coaxial connectors. Variations in both reflection and transmission characteristics are observed.

S21 log MAG
REF -0.660 dB
0.01 dB/

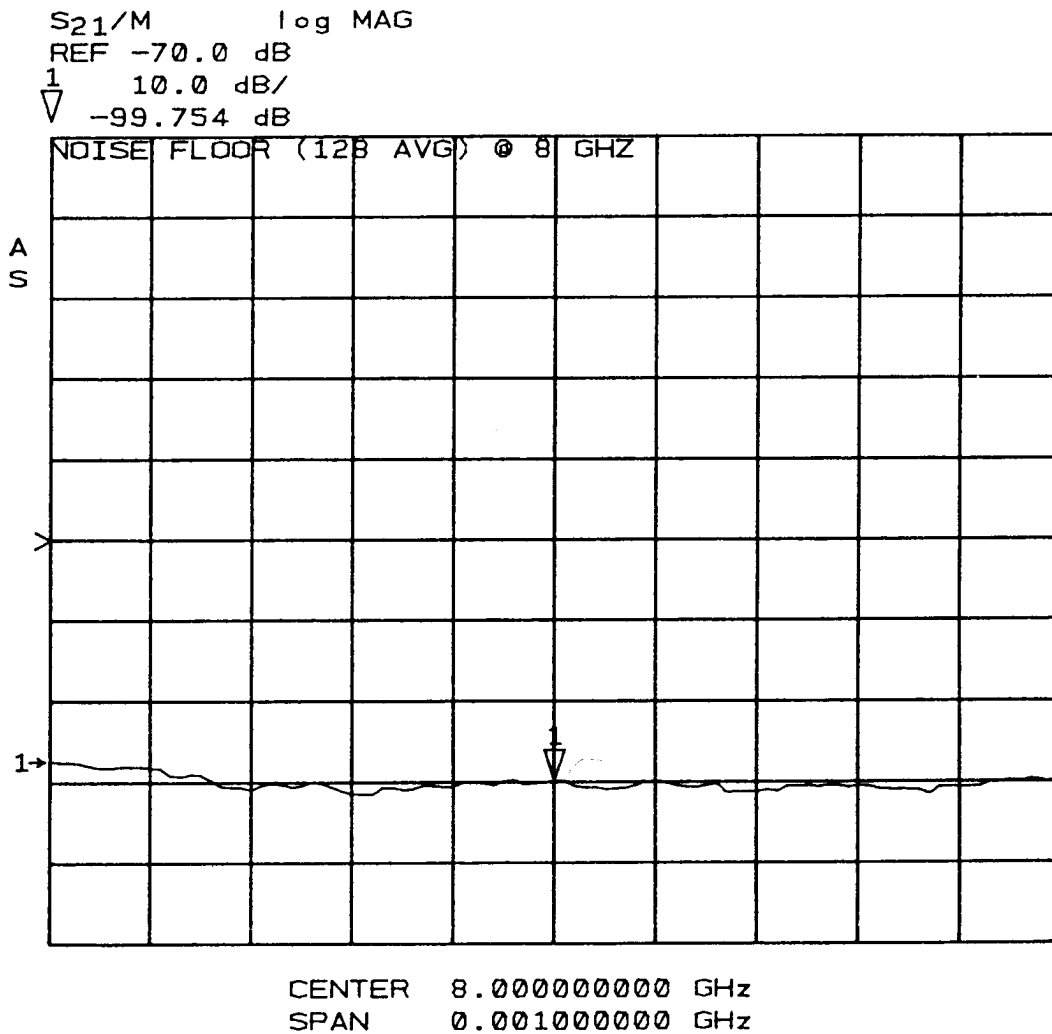


Nh - High Level Noise Plot - S21 Magnitude - 128 ave. at 8 GHz

This particular plot is an S21 measurement of a through connection taken at 8 GHz with an averaging index of 128. Note the fairly quiet trace characteristic on a .01 dB/division scale; without averaging the measurement would appear comparable on a .1 dB/division scale.

The primary source of error is the phase noise of the microwave signal source and the local oscillator.

This plot is typical of performance normally achieved with the 8512A test set. Note the .0009 dB RMS deviation; the specification is +/- .0015 dB RMS (.5 - 8 GHz) and +/- .002 dB RMS (8 - 18 GHz).



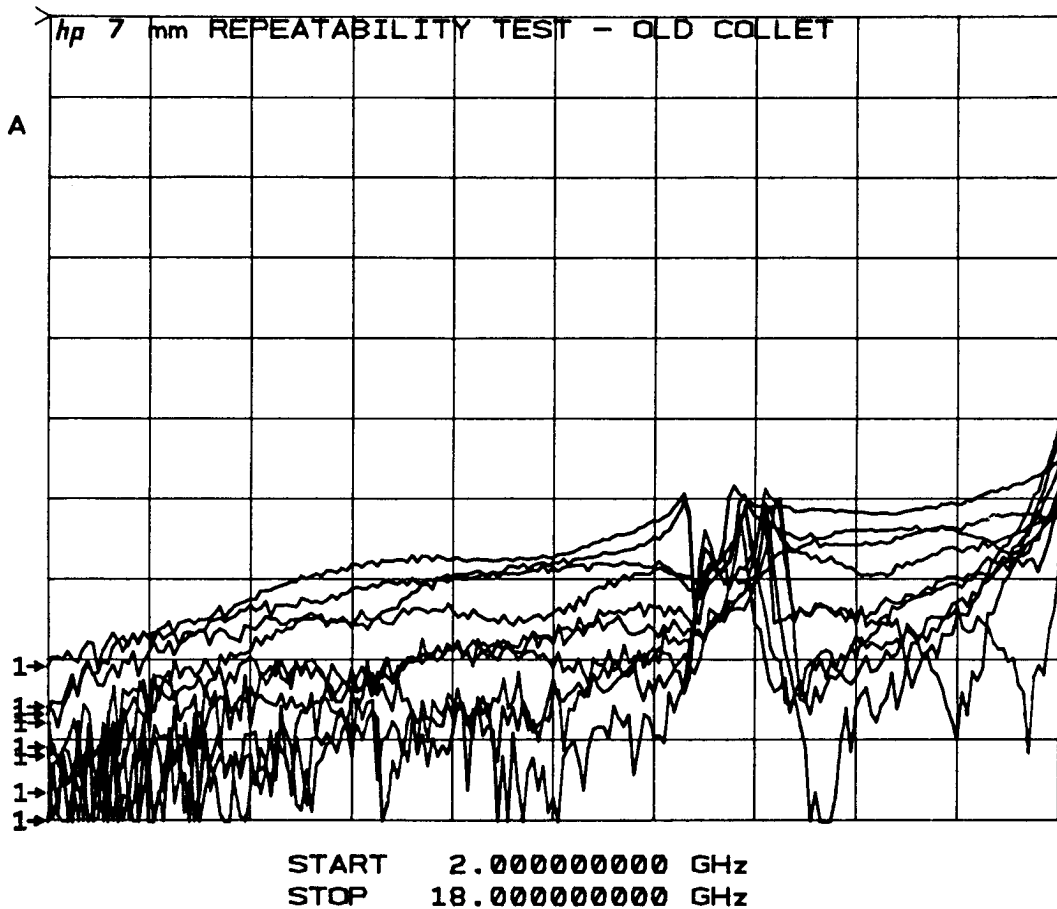
NI - Low Level Noise Plot - S₂₁ Magnitude (normalized) - 128 ave.

This plot shows an S₂₁ measurement with the ports terminated in fixed loads; it was made at 8 GHz with an averaging index of 128. In addition, smoothing was used to clearly define the mean value of the noise floor. Without averaging and smoothing the peaks of the noise floor would be about 25 dB higher.

The primary source of error is the noise figure of the sampling frequency converter.

This plot is typical of performance normally achieved with the 8512A test set. Note the measured noise floor approximately -99 dB from the reference level; the specification is -93 dB (.5 - 8 GHz) and -90 dB (8 - 19 GHz).

S11-M log MAG
REF 0.0 dB
10.0 dB/

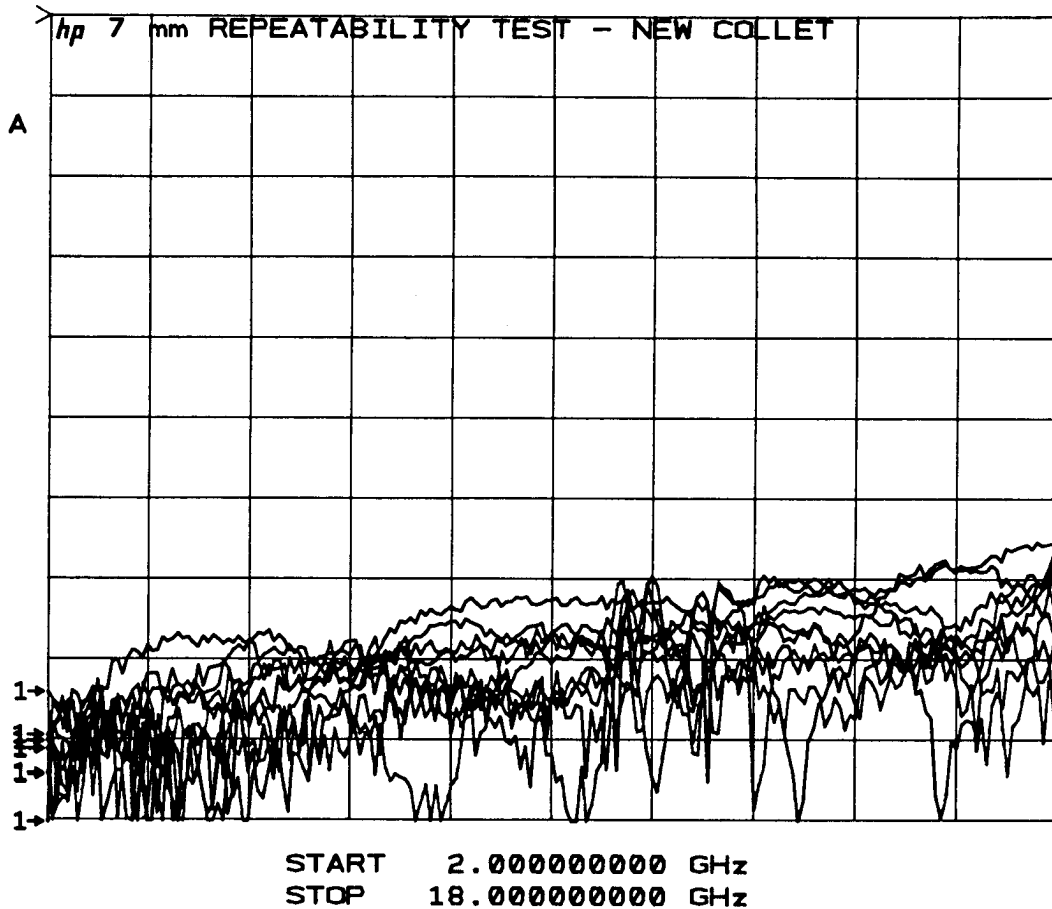


Rrl - 7 mm Connector Repeatability Test, 4 Slot Collets

This plot shows a connector test which extracts the reflection repeatability terms Rrl and Rr2. It is performed by measuring S11 of a fixed termination, storing the measurement in memory, disconnecting and reconnecting the termination, remeasuring S11, and then performing the S11 - M computation. The net effect is to measure the difference in return loss between two sequential connections of a well-matched device. This type of device is used to prevent contamination of the test by the transmission terms.

Note the areas of poor repeatability at 13 GHz caused by the 7 mm collet resonance and at 18 GHz caused by the first waveguide mode just out of band. This level of repeatability did not support the achievement of 50 dB effective directivity, and thus it was concluded that an improved connection interface must be developed.

S11-M log MAG
REF 0.0 dB
10.0 dB/



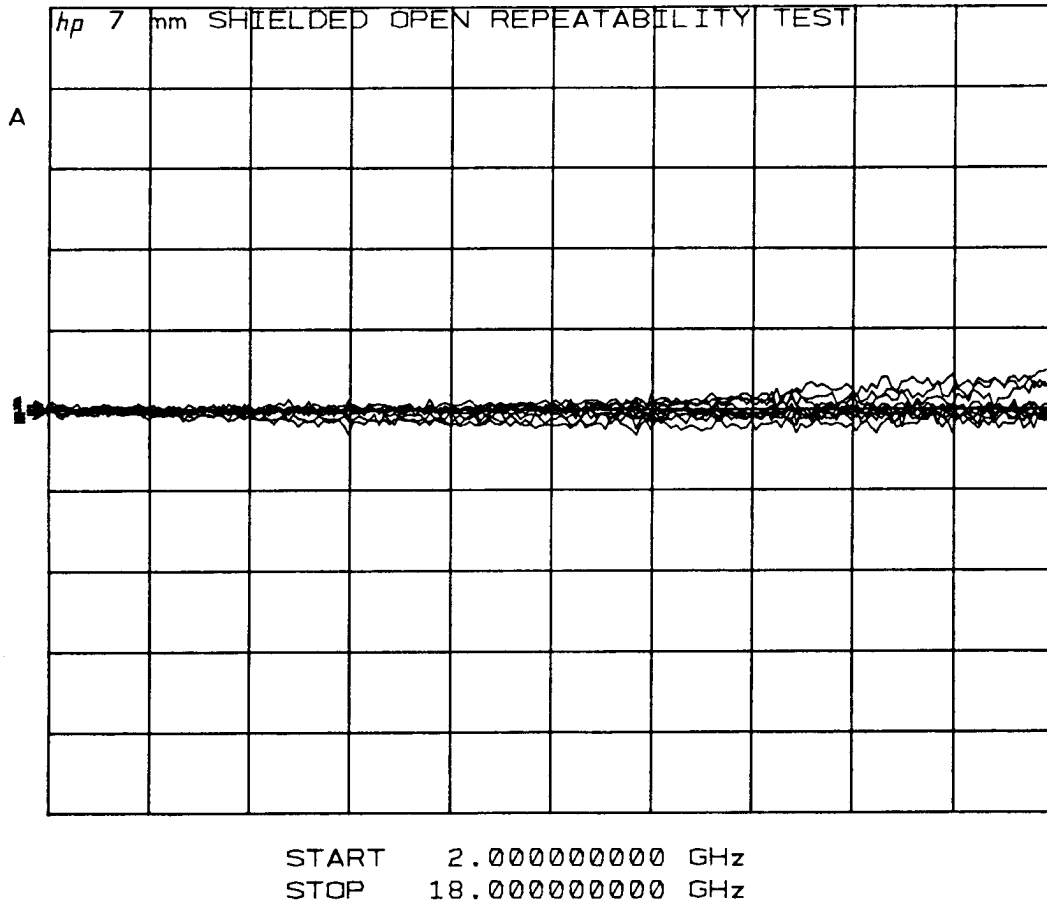
Rr1 - 7 mm Connector Repeatability Test, 6 Slot Collets

This plot shows a reflection repeatability test for a new 7 mm collet; the number of slots in the collet was increased from 4 to 6. The improvement shown is a result of an increased number of contact points and a reduced coupling inductance to the internal collet resonance. Further improvements are possible when the collet is in contact with a solid face center conductor, since no rotational ambiguity then exists between the contact faces.

The primary sources of error are the collet design, wear, user connection technique, and improper maintenance procedures. Secondary errors are caused by play in the locking mechanism and external forces applied to the connectors.

This plot is typical of performance normally achieved in 7 mm. The specification is -70 dB (.5 - 8 GHz) and -65 dB (8 - 18 GHz).

S11/M ∠
REF 0.0 °
100.0 m°/



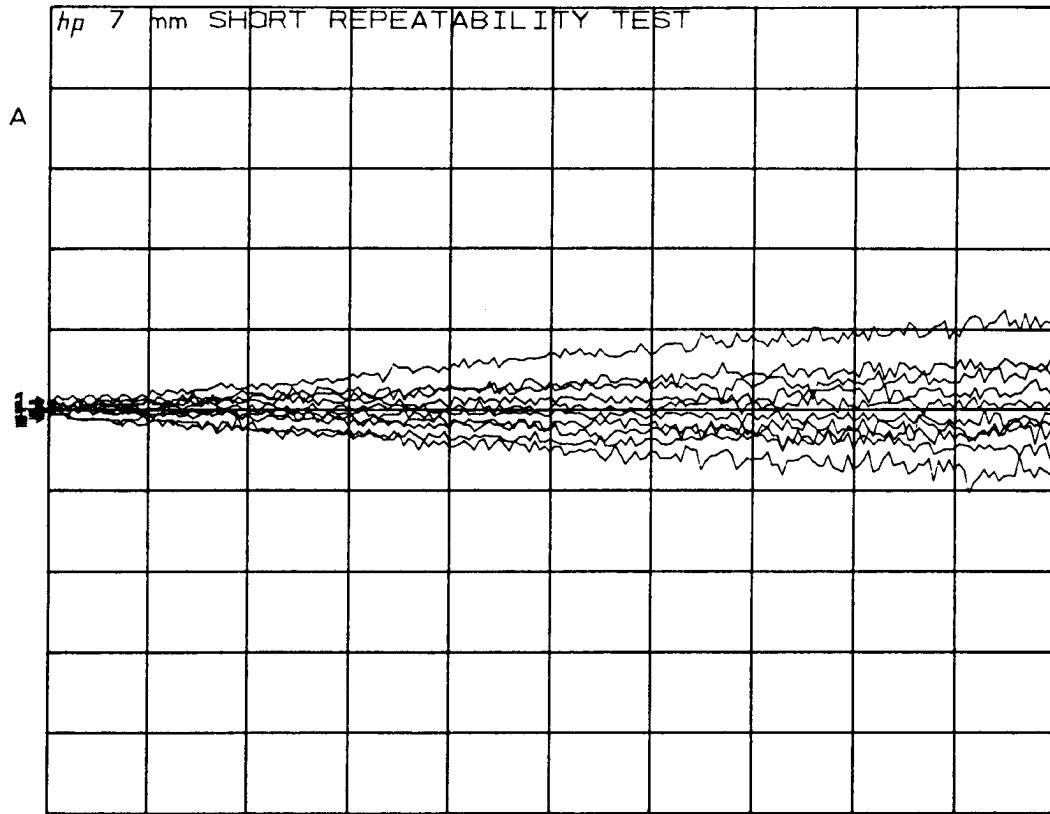
Shielded Open Repeatability Plot – S11/M Phase

This plot shows the phase repeatability of the new shielded open. This new reflection standard utilizes a dielectric plunger, set flush with the plane of the outer conductor, to press the collet of the test port to a repeatable position at the measurement plane. The older shielded open was merely an extension of the outer conductor, thus leaving the collet to assume an arbitrary extension depending on spring constant, wear, dirt, etc. Typical variations with the old open were of the order of several degrees.

Primary sources of error are wear of the plunger, wide temperature variations, user technique, and improper maintenance.

This plot is typical of performance normally achieved in 7 mm.

S11/M ∠
REF 0.0 °
100.0 m°/



START 2.000000000 GHz
STOP 18.000000000 GHz

Short Repeatability Plot – S11/M Phase

This plot shows the phase repeatability of the planar 7 mm short. Note the wider variations for the short test than with the open test. This results from the fact that the short generates a current peak at the interface, and thus variations in contact resistance and inductance are more significant; the open generates a current minimum.

Primary sources of error are wear, user technique, and improper maintenance.

This plot is typical of performance normally achieved in 7 mm.

Drift Error Sources

- f_d = Frequency
- Reflection Magnitude
- Reflection Phase
- Transmission Magnitude
- Transmission Phase

Drift Error Sources

Drift sources fall into two basic categories; frequency drift of the signal source and instrumentation drift. Instrumentation drift affects the magnitude and phase of both reflection and transmission measurements.

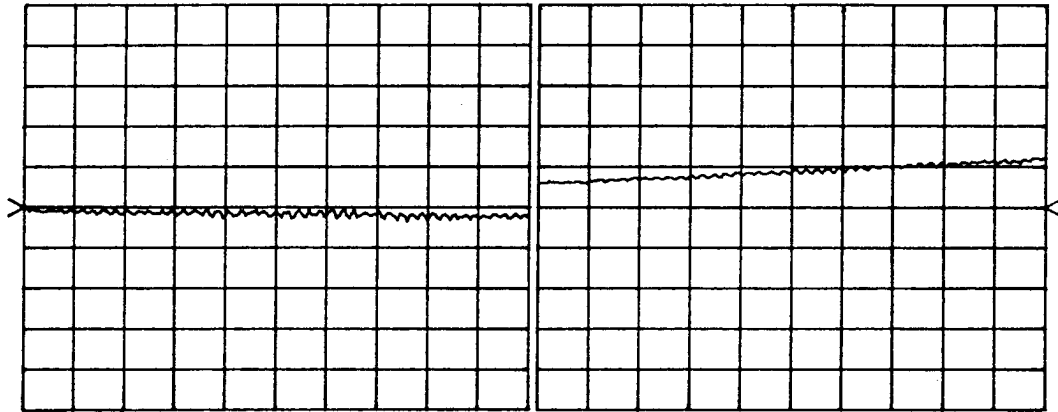
The primary causes for instrumentation drift are the thermal expansion characteristics of the interconnecting cables within the test set and the conversion stability of the microwave frequency converter.

S11/M log MAG
REF 0.0 dB
 0.1 dB/

S11/M ∠
REF 0.0 °
 1.0 °/

hp

SCALE
0.1 dB/div



START 0.500000000 GHz
STOP 18.000000000 GHz

Drift - 15 Deg. C. - Short on Test Port - S11/M Magnitude & Phase

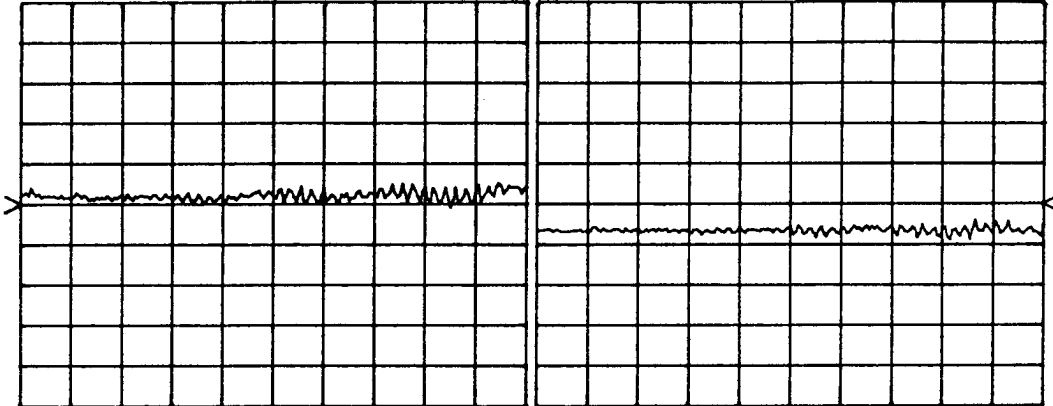
These plots were made by performing a simple reflection calibration at 25 Deg. Celsius with a short on the test port. The system temperature was then changed and stabilized at 15 Deg. Celsius. These plots of magnitude and phase drift are typical of reflection measurements made with a system based on the 8512A test set.

S₁₁/M log MAG
REF 0.0 dB
 0.1 dB/

S₁₁/M ∠
REF 0.0 °
 1.0 °/

lip

SCALE
 0.1 dB/div



START 0.500000000 GHz
STOP 18.000000000 GHz

Drift - 35 Deg. C. - Short on test Port - S₁₁/M Magnitude & Phase

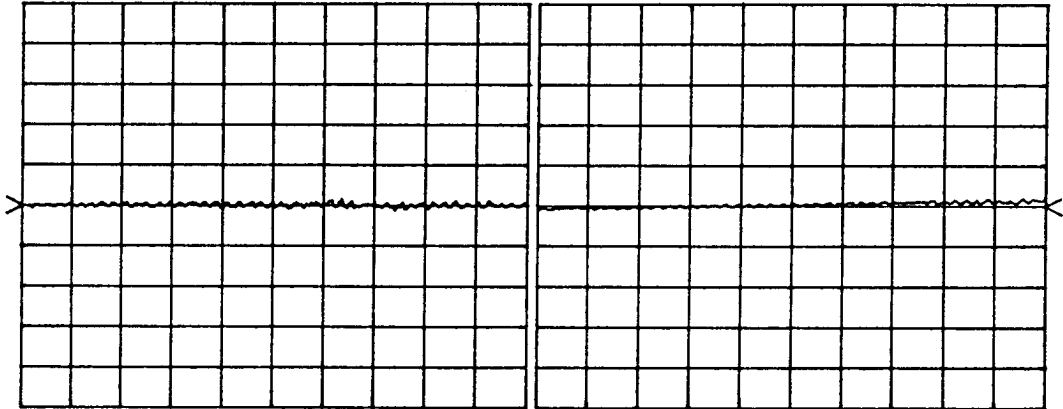
These plots show a continuance of the drift test. System temperature was changed from 15 to 35 Deg. Celcius and stabilized. Again these results represent typical drift performance for 8512A based system.

S11/M log MAG
REF 0.0 dB
 0.1 dB/

S11/M ∠
REF 0.0 °
 1.0 °/

lip

SCALE
 0.1 dB/div



START 0.500000000 GHz
STOP 18.000000000 GHz

Drift - Return to 25 Deg. C. - Short on Test Port - S11/M Mag. & Phase

These plots show a continuance of the drift test. System temperature was changed from 35 to 25 Deg. Celcius and stabilized. Notice that a returning to the starting temperature produced very good repeatability in both magnitude and phase. Again, these results represent typical drift performance for 8512A based systems.

In addition to thermal cycling tests, a longer term aging test was performed with very favorable results. An 8512A based system was placed in a standards laboratory where temperature is controlled to +/- .5 Deg. Celcius. A normal one port reflection calibration was performed and periodically checked over a one month interval. It was found that short and open reflection standards were consistently measured to +/- .01 dB and +/- .1 degree, thus indicating virtually no long term aging effects.

Frequency Dependent Errors

$$\text{Let } f = f_0 + F \pm F_d$$

f = actual frequency

f_0 = nominal frequency

F = Systematic Frequency Error

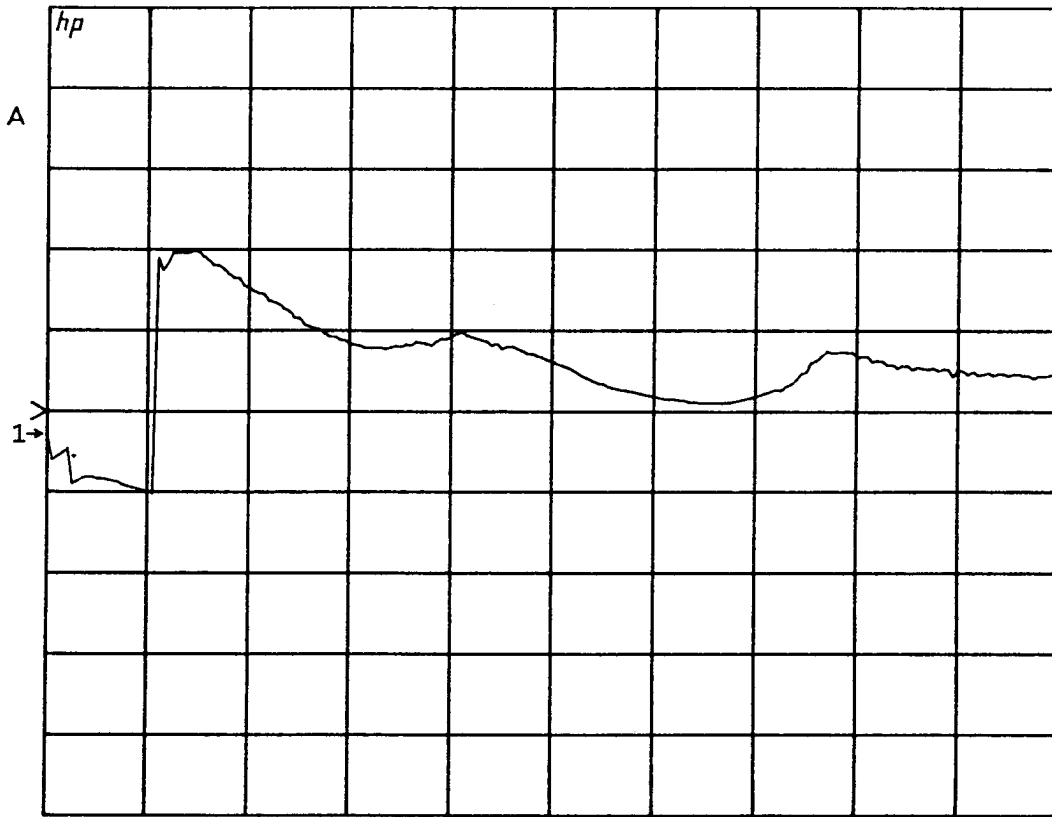
F_d = Frequency Drift Error

Frequency Sensitivity	F	F _d
Calibration Devices	Very Small	Very Small
System Hardware	None	Moderate/Large
Device Under Test	Device Dependent	Device Dependent

Frequency Dependent Errors

Except for one case, it is found that absolute frequency accuracy and frequency drift have an impact on measurement accuracy in proportion to the frequency sensitivity of the hardware in question. The exception is that system hardware is immune to absolute frequency errors, since calibration and measurement are performed with the same frequency set. However, frequency drift can be a serious problem for system hardware, since frequency sensitivity can be quite high as a result of long cables within the test set. Calibration devices contribute very little problem in either situation as a result of very low frequency response sensitivities. Test devices can vary widely -in sensitivity and thus must be individually considered; errors will be in direct proportion to the response of the device (dB/Hz. or Deg./Hz.).

S₂₁/M ∠
 REF 0.0 °
 10.0 °/

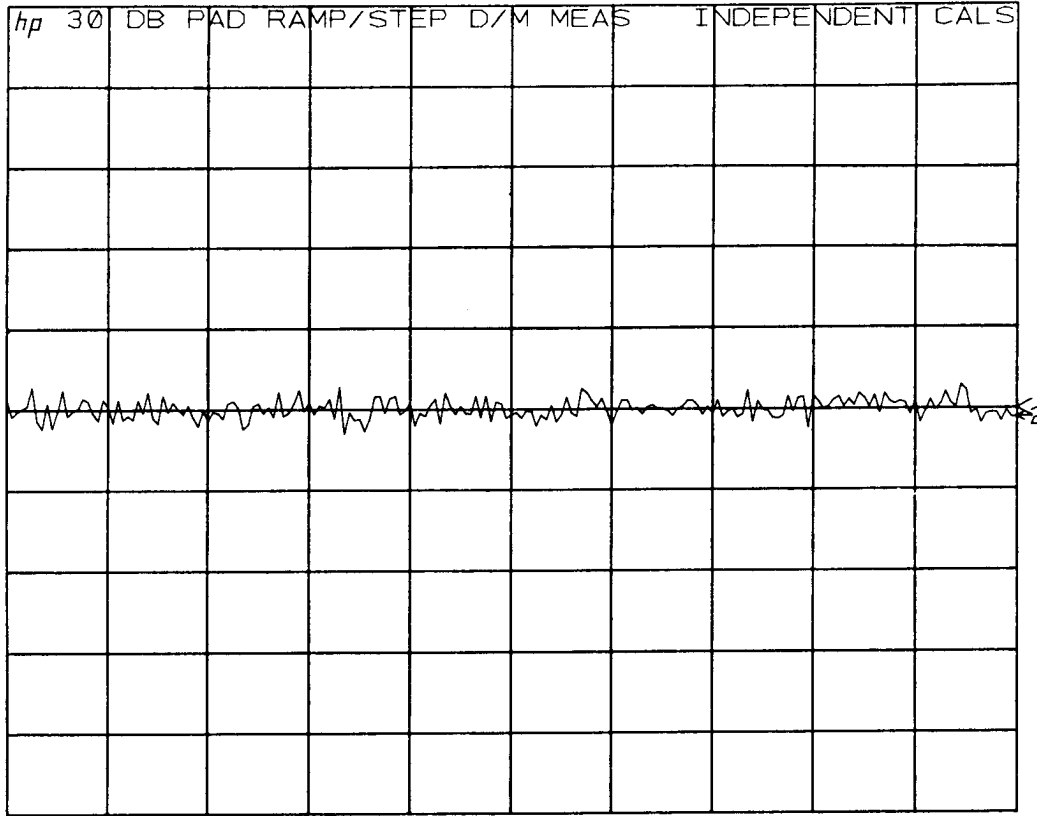


START 0.500000000 GHz
 STOP 18.000000000 GHz

30 cm. Airline - S₂₁/M Phase - Step vs. Ramp - Independent Cals.

This test shows a comparison of the transmission phase of a 30 cm. airline measured in the Step Sweep mode (synthesized) and the Ramp Sweep mode (voltage tuned) utilizing an 8340A sweeper. In both cases, system calibration was performed in the same mode as the measurement. A vector ratio of the two measurements shows the phase error which results from the frequency inaccuracies of the Ramp Sweep mode. It is easy to note that a frequency discontinuity exists at the boundary of the heterodyne and fundamental bands. Also the characteristic shape of the fundamental band is partially repeated in the harmonic bands. Dynamic effects of the harmonic change points of the network analyzer may also be seen within the heterodyne band. Based on this example, it is straightforward to see that precision measurements of long transmission lines will require a synthesized source.

S₂₁/M log MAG
 REF 0.0 dB
 0.1 dB/

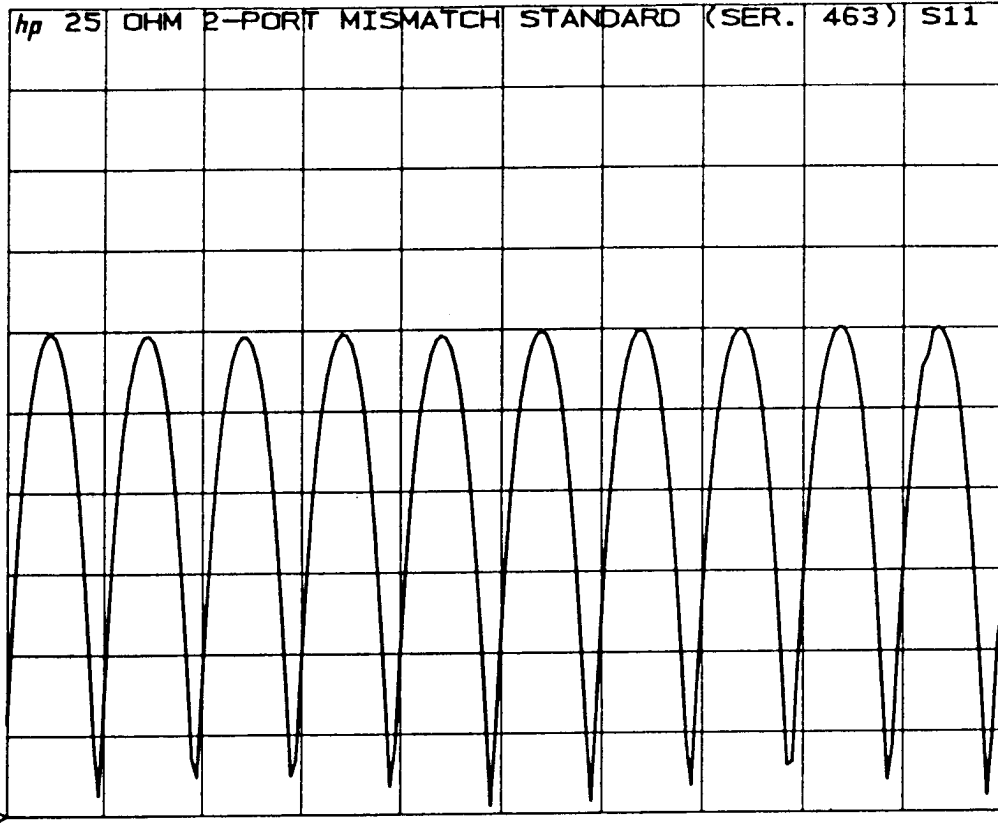


START 0.100000000 GHz
 STOP 20.100000000 GHz

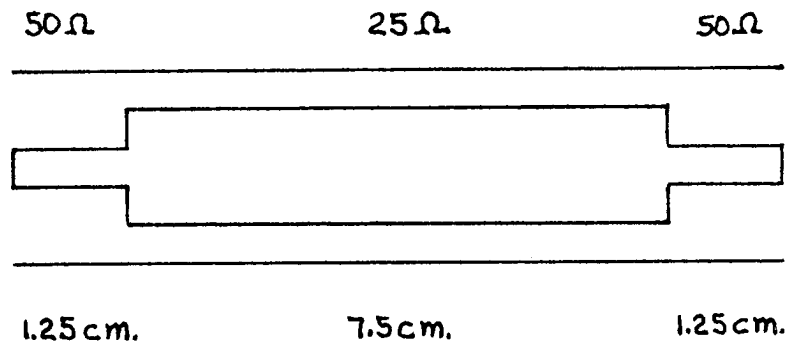
30 dB pad - S₂₁/M Magnitude - Step vs. Ramp - Independent Cals.

This test shows a comparison of the transmission magnitude of a 30 dB fixed attenuator measured in the Step Sweep mode (synthesized) and the Ramp Sweep mode (voltage tuned) utilizing an 8340A sweeper. In both cases, system calibration was performed in the same mode as the measurement. A vector ratio of the two measurements shows virtually no magnitude errors resulting from the frequency inaccuracies of the Ramp Sweep mode; trace ripple is caused by noise and is typical of measurements at this level. Based on this example, it may be seen that devices with smooth broadband frequency responses can be accurately measured utilizing sources in the Ramp Sweep mode.

M only LINEAR
REF 0.0 Units
100.0 mUnits/



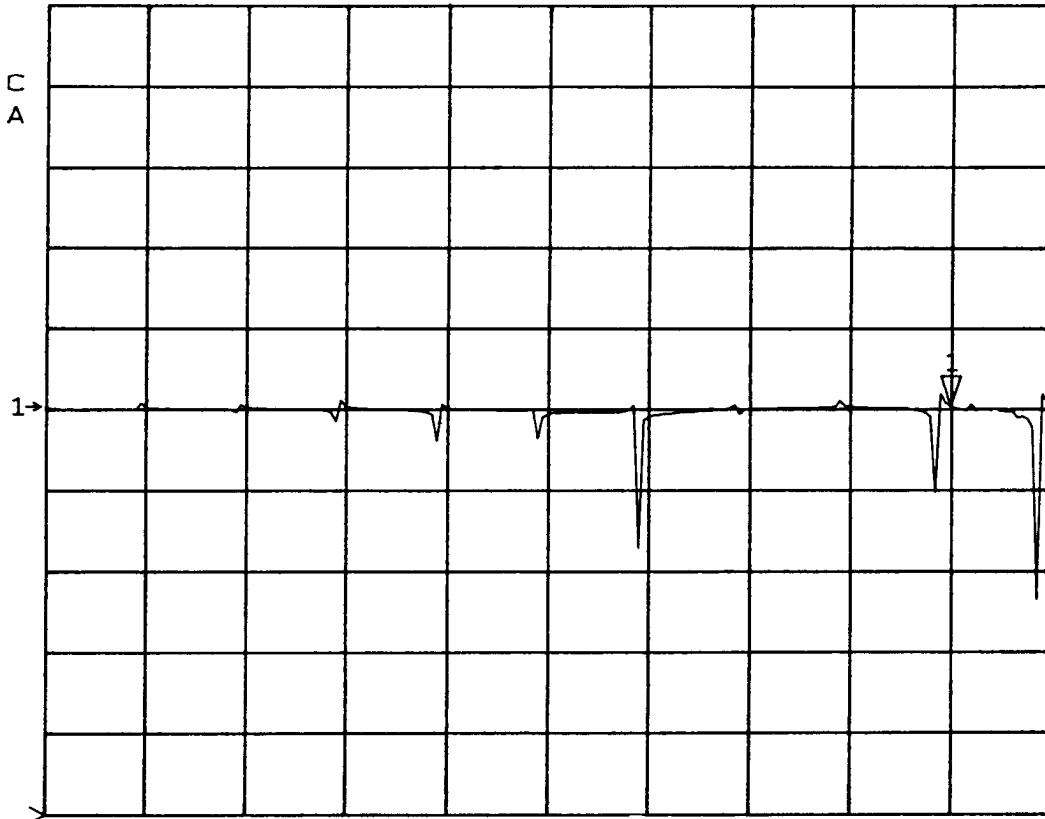
START 0.100000000 GHz
STOP 20.100000000 GHz



25 Ohm 2-Port Impedance Std. - S11 Magnitude

This measurement shows S11 (linear magnitude) of a two-port mismatch impedance standard. It is notable because of the periodic response with areas of both small and large frequency sensitivity.

S₁₁/M LINEAR
 REF 500.0 mUnits
 1 100.0 mUnits/
 ▽ 1.0034 U.



START 0.100000000 GHz
 STOP 20.100000000 GHz

25 Ohm 2-Port Impedance Std. - S₁₁/M - Step vs. Ramp - Independent Cals.

This test shows a comparison of linear reflection magnitude of a two-port mismatch standard measured in the Step Sweep mode (synthesized) and the Ramp Sweep mode (voltage tuned) utilizing an 8340A sweeper. In both cases, system calibration was performed in the same mode as the measurement. A vector ratio of the two measurements shows the magnitude error which results from the frequency inaccuracies of the Ramp Sweep mode. In this measurement it is easy to see how frequency accuracy problems are aggravated by test devices with regions of highly responsive characteristics.

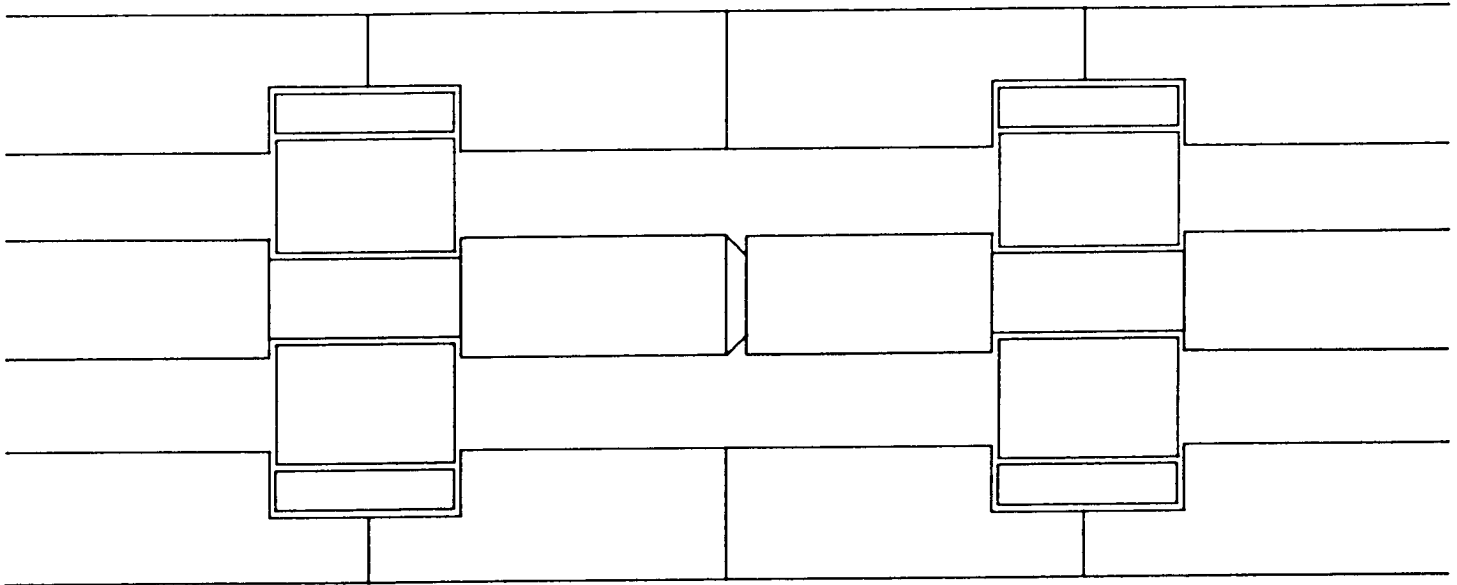
Sources of Operator Error

- Connection Technique
- Maintenance of Connector Dimensions
- Maintenance of Contact Surfaces

Sources of Operator Error

In addition to hardware, the list of error sources must include the operator. It can be true that the operator is the largest source of error in the system.

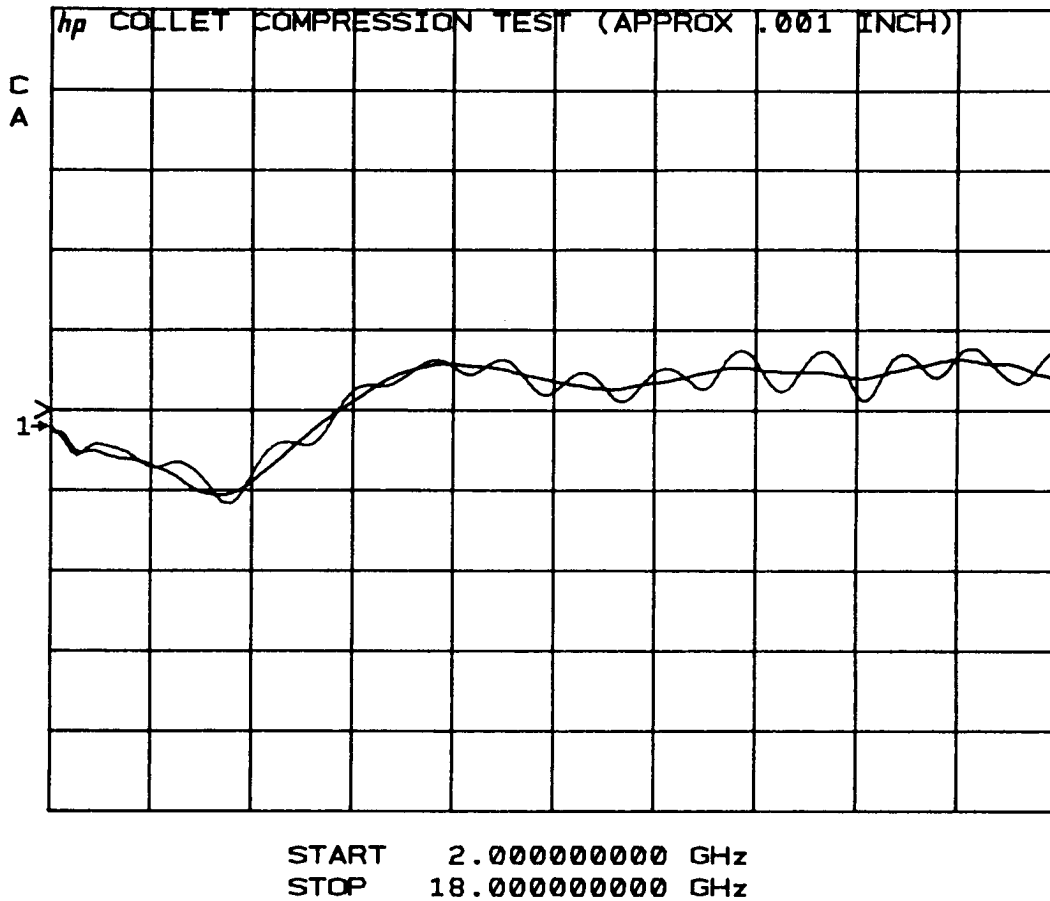
- | | |
|------------------------|--|
| Connection technique - | counterrotation, torque limits, flush setting of sliding load center conductors, handling procedures for beadless airlines |
| Connector dimensions - | axial alignment, shoulder setback, pin diameter, collet extension |
| Contact surfaces - | cleaning procedures, inspection procedures for scratches, worn plating, rough seating |



7 mm Flush Interface

This pictorial illustrates a simplified view of a 7mm connection between the test port (right side) and a calibration device (left side). Prior procedure with older network analyzers called for the center conductor of the sliding load to be installed on the test port in such a way that the collet was fully compressed. While this may have generated a low mismatch connection, it was not the condition which exists when connected to a test device; such a connection is represented in the pictorial. Thus a systematic error could be created as a result of the installation technique used with the sliding load.

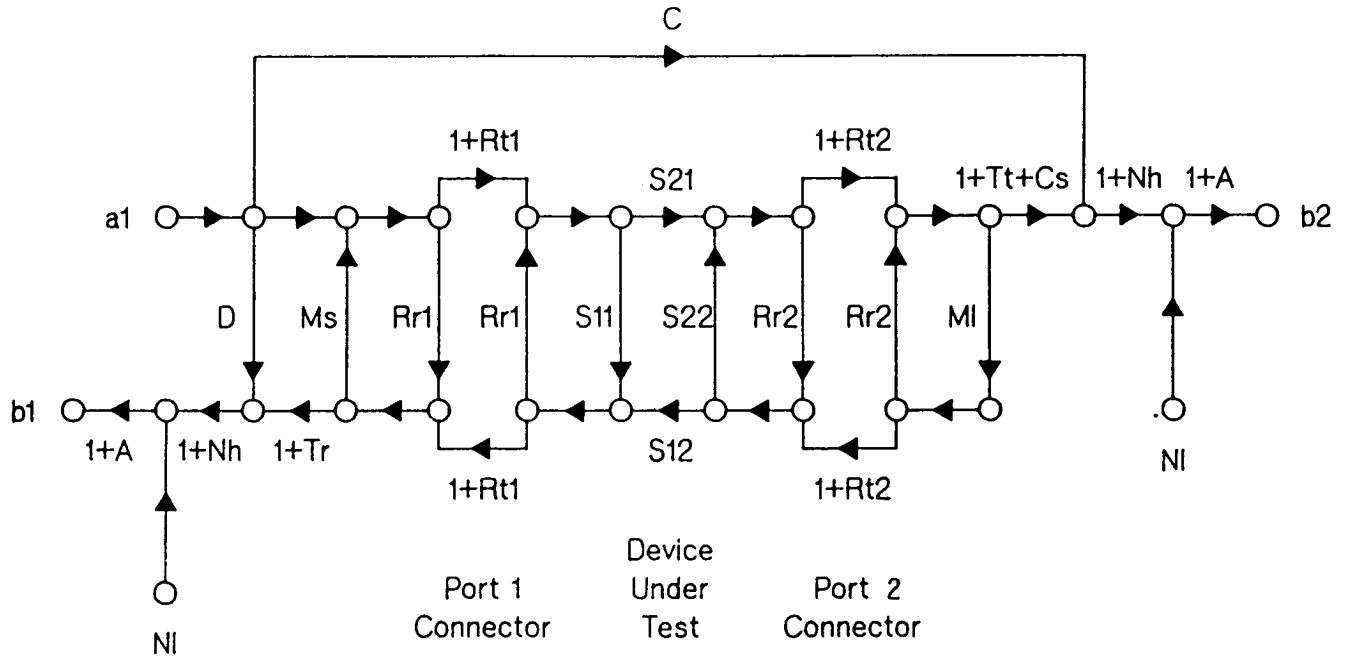
S22 & M log MAG
 REF -40.0 dB
 5.0 dB/



S22 & M - Flush & Compressed Collet - 7 mm Sliding Load on Test Port

In order to generate this pictorial, a normal one port reflection calibration was performed. The shoulder of the sliding load center conductor was set flush with the outer conductor and locked in position prior to installation on the test port. At the conclusion of the calibration process, the sliding load was left engaged to the test port and was merely measured as a fixed load (the smoother trace). As can be seen, the element match of the sliding load appears to be approximately -40 dB. The center conductor locking mechanism was then loosened, and the center conductor was pressed in, fully compressing the test port collet. The center conductor was again locked in position and the element match was remeasured (trace with ripples). Note the dramatic change as a result of compressing the collet by only .001 inch. Obviously, a consistent condition of the test port for both calibration and measurement is critical for high performance.

8510A / 8512A Error Model



8510 / 8512 Error Model

This error model shows the relationship of the various error sources and may be used to analyze overall performance. Note the appearance of the dynamic accuracy, noise errors, and connector repeatability terms which appear on both the reflection and transmission portions of the model. On the reflection side the familiar directivity, source match, and tracking appear. The crosstalk error spans the model indicating the leakage path around the test device. On the transmission side the familiar load match and tracking terms are joined by the cable stability error.

8510 / 8512 Performance Specifications

	8.0 GHz	18.0 GHz
=====	=====	=====
D = residual directivity	-50.0 dB	-50.0 dB
Ms = residual source match	-40.0 dB	-40.0 dB
Tr = residual reflection tracking	+-.050 dB	+-.050 dB
C = residual crosstalk	-90.0 dB	-90.0 dB
Ml = residual load match	-40.0 dB	-40.0 dB
Tt = residual transmission tracking	+-.015 dB	+-.030 dB
Cs = cable stability (0.1 deg/GHz)	0.8 deg	1.8 deg
Nh = high level noise (rms)	+-.0015 dB	+-.0020 dB
Nl = low level noise (rms)	-93.0 dB	-90.0 dB
Rr1 = port-1 reflection repeatability	-70.0 dB	-65.0 dB
Rt1 = port-1 transmission repeatability	-70.0 dB	-65.0 dB
Rr2 = port-2 reflection repeatability	-70.0 dB	-65.0 dB
Rt2 = port-2 transmission repeatability	-70.0 dB	-65.0 dB
Ea = I.F. autorange gain error (12 dB)	+-.005 dB	+-.005 dB
Ea = I.F. autorange gain error (24 dB)	+-.005 dB	+-.005 dB
Ea = I.F. autorange gain error (36 dB)	+-.010 dB	+-.010 dB
Ea = I.F. autorange gain error (48 dB)	+-.010 dB	+-.010 dB
Eco = compression error; .100 dB at	-10.0 dBm	-10.0 dBm
Eci = circularity error	+-.003 dB	+-.003 dB
Edc = effective D.C. offset error	-100.0 dBm	-100.0 dBm
El = I.F. linearity error	+-.003 dB	+-.003 dB
Er = I.F. residual signal error	-120.0 dBm	-120.0 dBm
Gs = sampler gain	-3.0 dB	-4.0 dB
Incremental Phase Linearity = +- .001 degrees/degree, <.02 deg. total		
R = reference level (typ @ 20 MHz I.F.)	-22.0 dBm	-26.0 dBm

Reflection Magnitude Uncertainty

$$E_{rm} = S_r + \sqrt{W_r^2 + X_r^2 + Y_r^2 + Z_r^2}$$

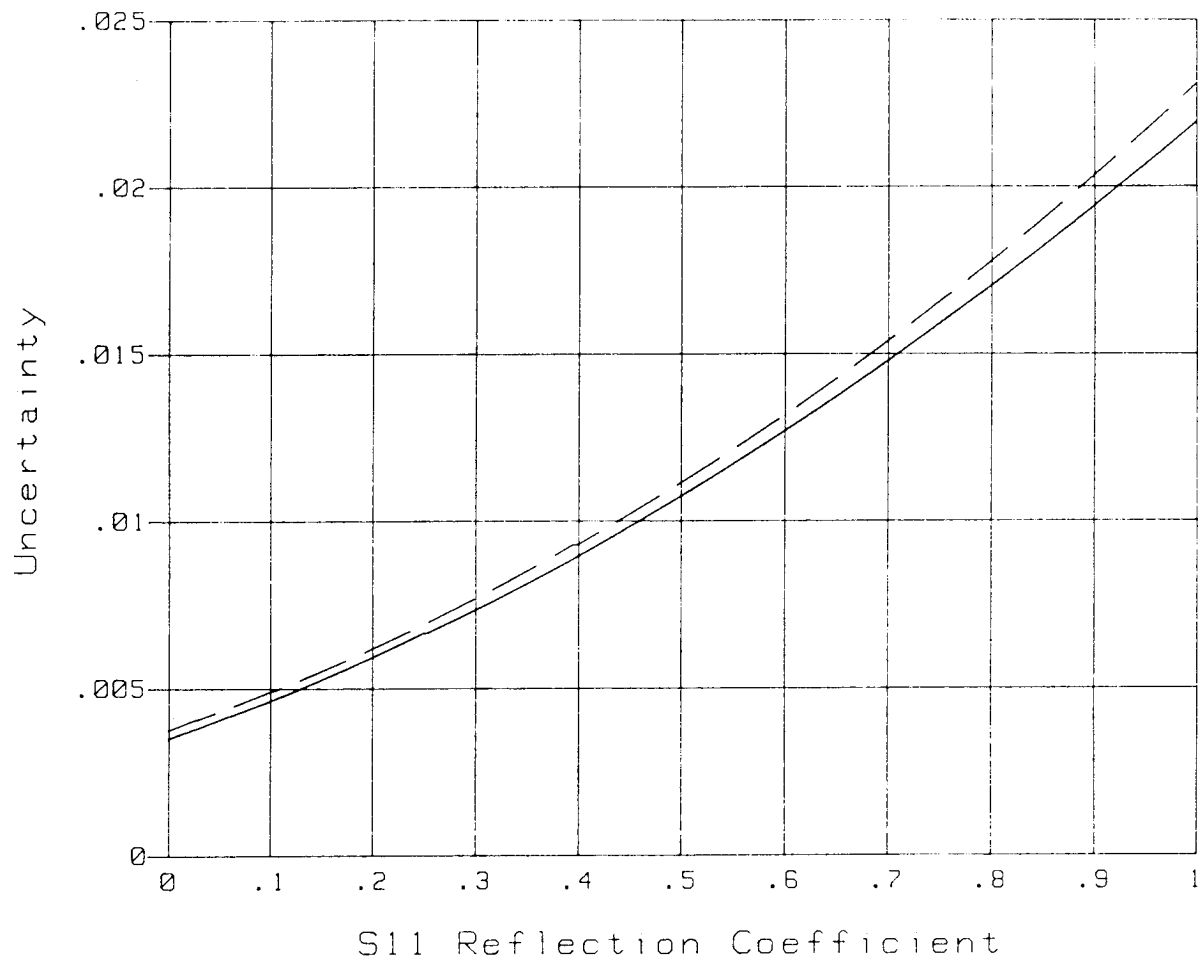
$$E_{rm} (\log) = 20 \cdot \log(1 \pm E_{rm}/S_{11})$$

- $S_r = D + T_r \cdot S_{11} + M_s \cdot S_{11}^2 + M_l \cdot S_{21} \cdot S_{12} + A \cdot S_{11}$ (Sys Error)
- $W_r = 3 \cdot N_l$
(Random Low Level Noise)
- $X_r = 3 \cdot N_h \cdot S_{11}$
(Random High Level Noise)
- $Y_r = 2 \cdot R_{t1} \cdot S_{11} + R_{r1} \cdot S_{11}^2 + R_{r1}$
(Random Port 1 Repeatability)
- $Z_r = R_{r2} \cdot S_{21} \cdot S_{12}$
(Random Port 2 Repeatability)

Reflection Magnitude Uncertainty

An analysis of the error model yields an equation for the reflection magnitude uncertainty. It may be seen that the four groups of terms under the radical are random in character, and thus are combined on an RSS basis. The terms in the systematic error group are combined on a worst case vector basis. In all cases, the error terms are treated as linear absolute magnitudes. Note that many of the terms involve the measured S-parameters. Thus it is found that the magnitude of many of the errors depends upon the level of the test signal. In order to simplify the equations to generate a performance overview, it has been traditional to set $S_{21} = S_{12} = 0$. This treats the test device as a one port and makes a simple graphical presentation possible (shown in the next pictorial). In the event that S_{21} and S_{12} are not zero, the full equations must be utilized to predict overall performance.

S11 Magnitude Uncertainty (Linear)



Reflection Magnitude Uncertainty Plot - S11 Linear Magnitude

This plot shows measurement uncertainty as a function of reflection magnitude. It assumes that the test device is a one-port ($S_{21} = S_{12} = 0$). At low reflections, the performance is limited by effective directivity, connector repeatability, and low level noise. At high reflections, source match, high-level noise, and tracking tend to limit performance.

(solid = 8 GHz, dashed = 18 GHz)

Transmission Magnitude Uncertainty

$$E_{tm} = S_{t1} + \sqrt{W_{t1}^2 + X_{t1}^2 + Y_{t1}^2 + Z_{t1}^2}$$

$$E_{tm} (\log) = 20 \cdot \log(1 \pm E_{tm}/S_{t1})$$

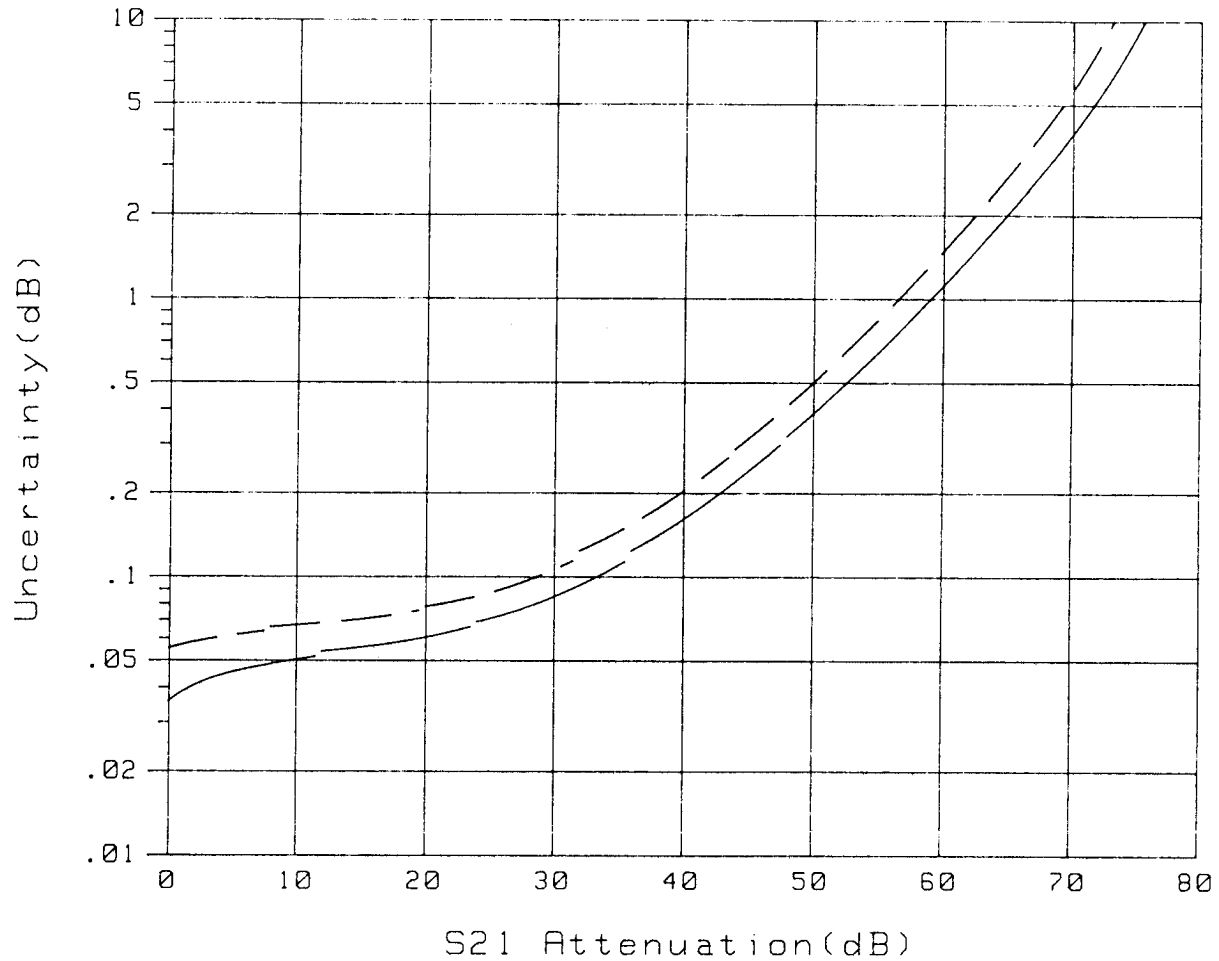
- $S_{t1} = C + T_{t1} \cdot S_{21} + M_s \cdot S_{11} \cdot S_{21} + M_I \cdot S_{22} \cdot S_{21} + A \cdot S_{21}$ (Sys Error)
- $W_{t1} = 3 \cdot N_I$
(Random Low Level Noise)
- $X_{t1} = 3 \cdot N_h \cdot S_{21}$
(Random High Level Noise)
- $Y_{t1} = R_{t1} \cdot S_{21} + R_{r1} \cdot S_{11} \cdot S_{21}$
(Random Port 1 Repeatability)
- $Z_{t1} = R_{t2} \cdot S_{21} + R_{r2} \cdot S_{22} \cdot S_{21}$
(Random Port 2 Repeatability)

Transmission Magnitude Uncertainty

An analysis of the error model yields an equation for the transmission magnitude uncertainty. It may be seen that the four groups of terms under the radical are random in character, and thus are combined on an RSS basis. The terms in the systematic error group are combined on a worst case vector basis. In all cases, the error terms are treated as linear absolute magnitudes. Note that many of the terms involve the measured S-parameters. Thus it is found that the magnitude of many of the errors depends upon the level of the test signal. In order to simplify the equations to generate a performance overview, it has been traditional to set $S_{11} = S_{22} = 0$. This treats the test device as a perfectly matched device and makes graphical presentation possible (shown in the next pictorial). In the event that S_{11} and S_{22} are not zero, the full equations must be utilized to predict overall performance.

(solid = 8 GHz, dashed = 18 GHz)

S21 Magnitude Uncertainty (dB)



Transmission Magnitude Uncertainty Plot - S21 Log Magnitude

This plot shows measurement uncertainty as a function of transmission magnitude. It assumes that the test device is perfectly matched ($S_{11} = S_{22} = 0$). At high signal levels, performance is limited by high-level noise, tracking, connector repeatability, and dynamic accuracy effects. At low signal levels, performance is limited by low-level noise, and crosstalk.

(solid = 8 GHz, dashed = 18 GHz)

Reflection Phase Uncertainty

$$E_{rp} = \text{Arcsin}(E_{rm}/S_{11})$$

Transmission Phase Uncertainty

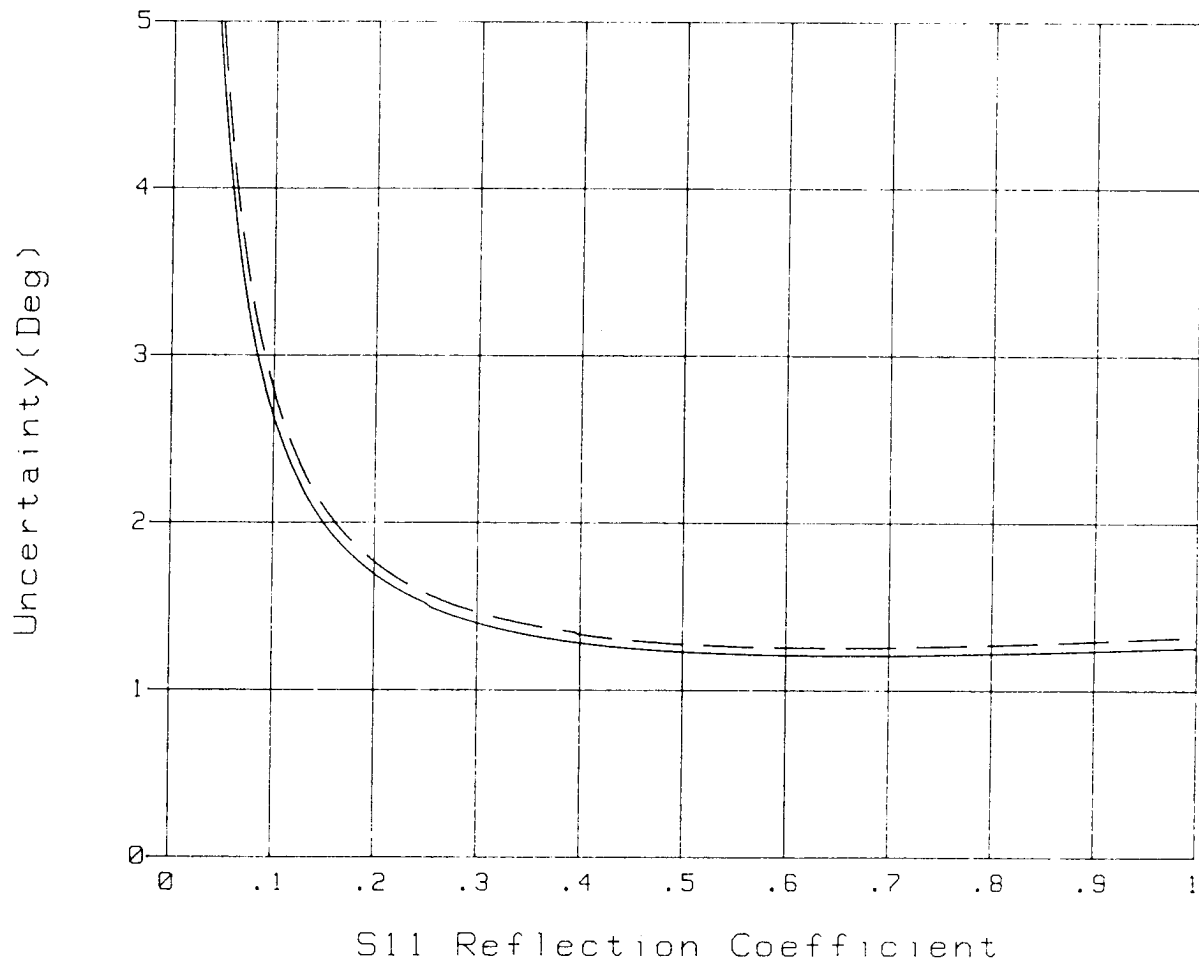
$$E_{tp} = \text{Arcsin}(E_{tm}/S_{21}) + C_s * f \text{ (GHz)}$$

Reflection & Transmission Phase Uncertainty

Reflection phase uncertainty is determined from a comparison of the magnitude uncertainty with the test signal magnitude. The worst case phase angle is computed.

Transmission phase uncertainty is calculated in the same way but with contribution of cable phase stability added on a worst-case basis.

S11 Phase Uncertainty (Deg)

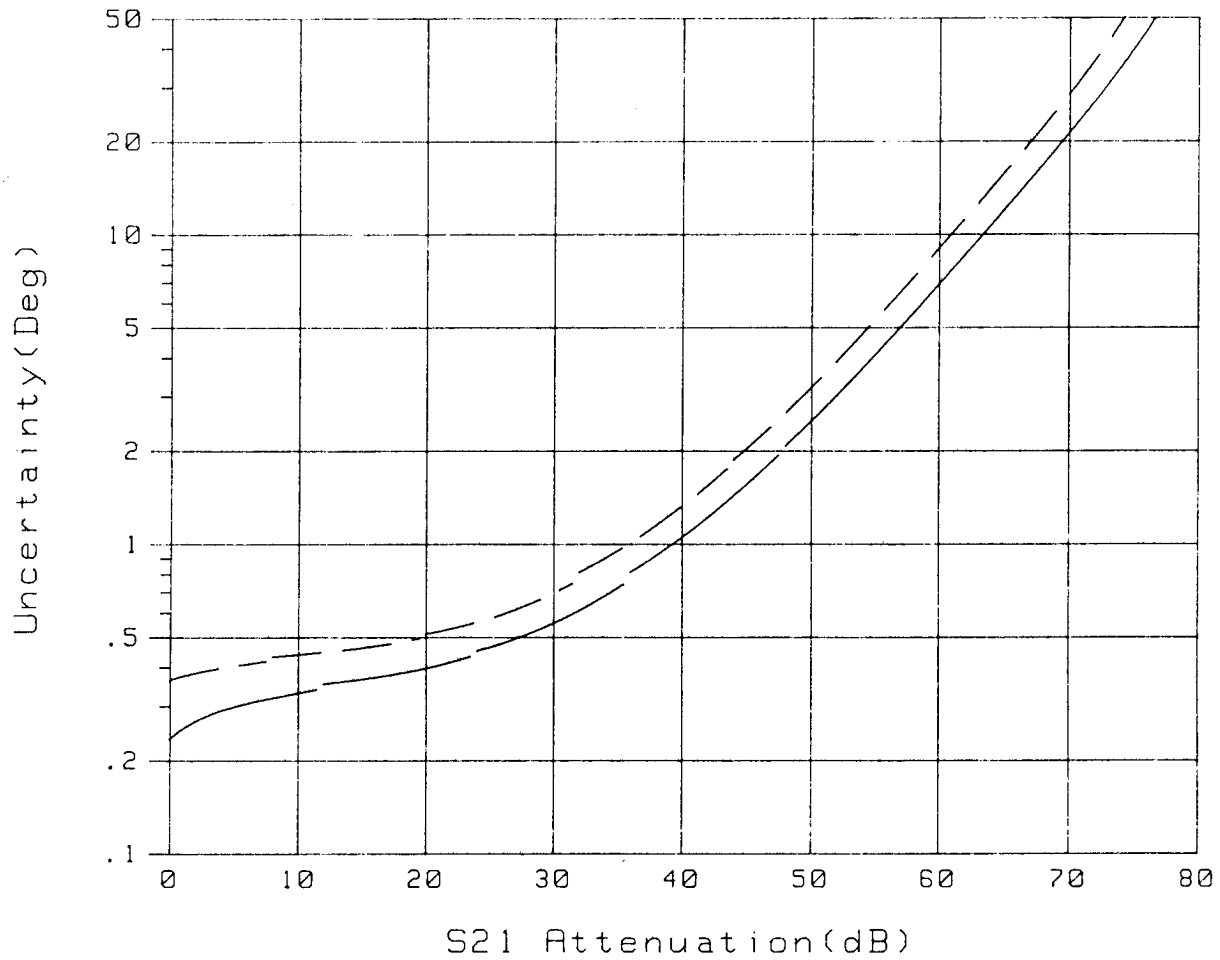


Reflection Phase Uncertainty Plot – S11 Phase

This plot shows phase uncertainty as a function of reflection magnitude. It assumes that the test device is a one-port ($S_{21} = S_{12} = 0$). As S_{11} decreases, the finite magnitude uncertainty, coupled with a vanishingly small reflection coefficient, causes the phase uncertainty to grow (it is difficult to measure the phase of a zero length vector!).

(solid = 8 GHz, dashed = 18 GHz)

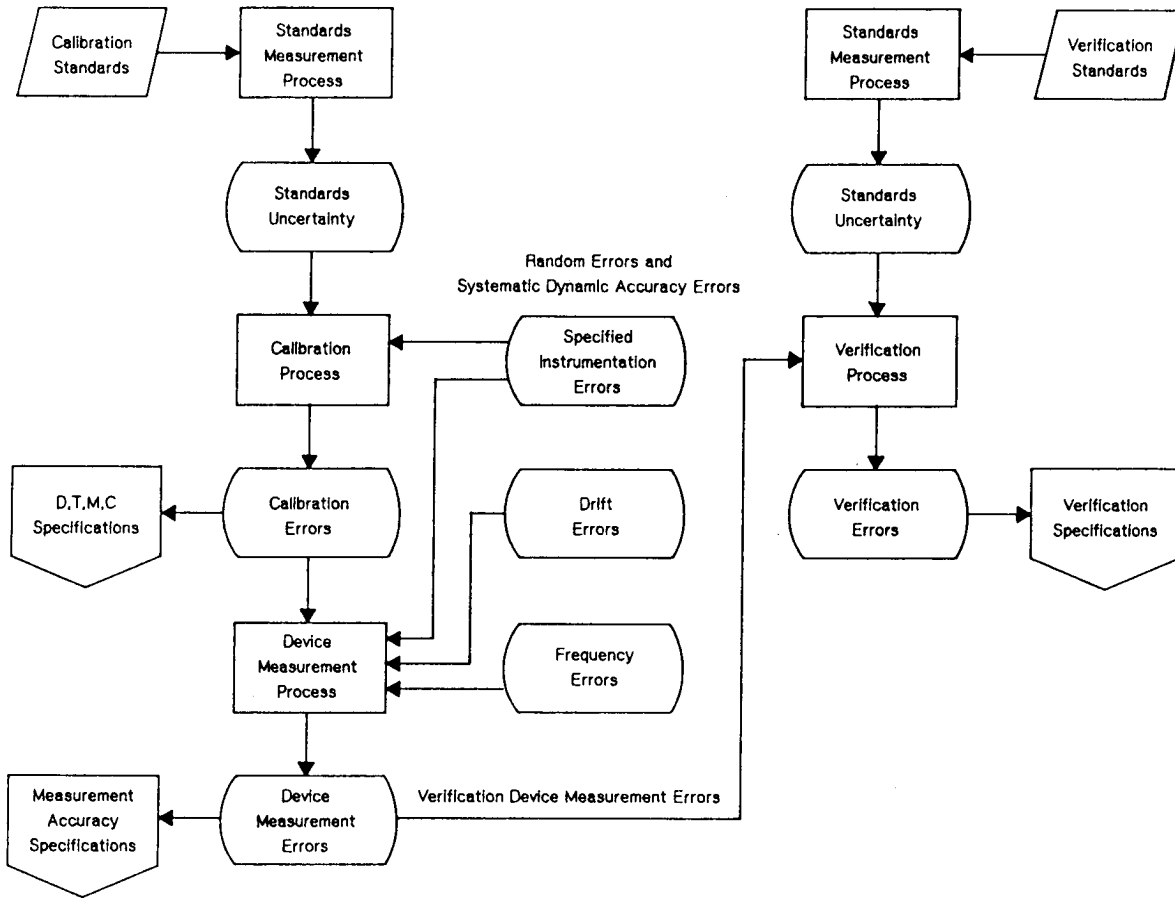
S21 Phase Uncertainty (Deg)



Transmission Phase Uncertainty Plot - S21 Phase

This plot shows phase uncertainty as a function of transmission magnitude. It assumes that the effects of cable flexing are zero and that the test device is perfectly matched ($S_{11} = S_{22} = 0$). At high signal levels, performance is limited by high-level noise, tracking, connector repeatability, and dynamic accuracy effects. At low signal levels, performance is limited by low-level noise, and crosstalk.

Specification Generation Flowgraph

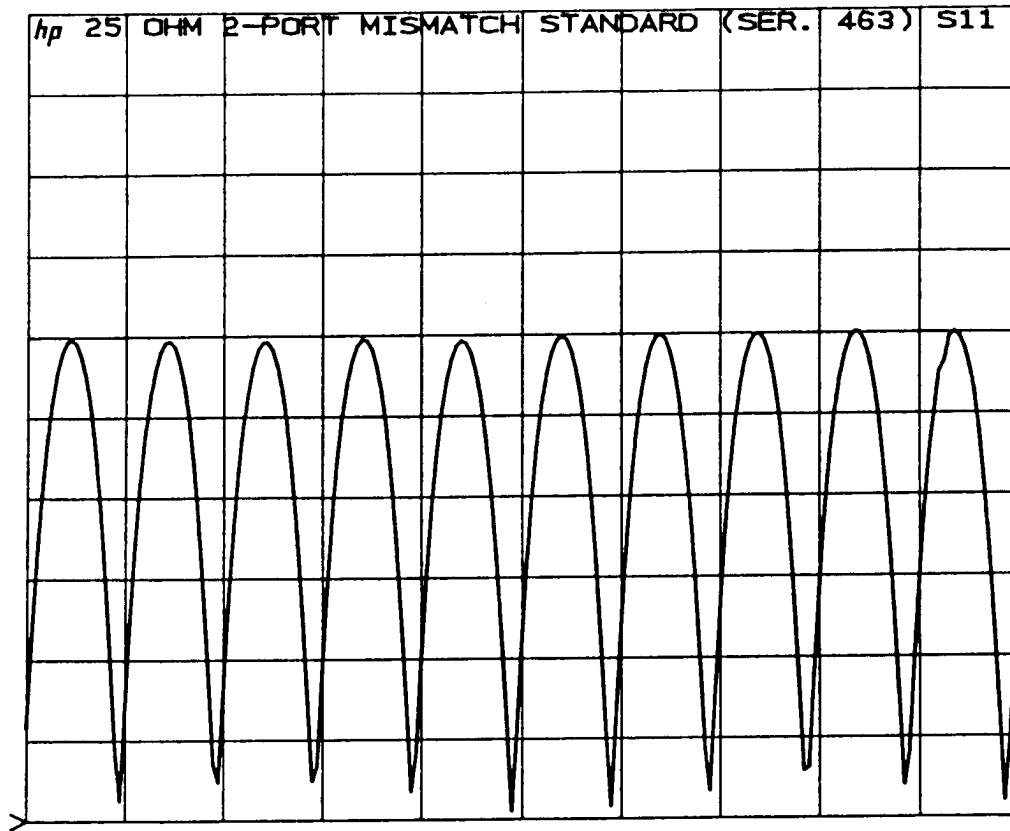


Specification Generation Flowgraph

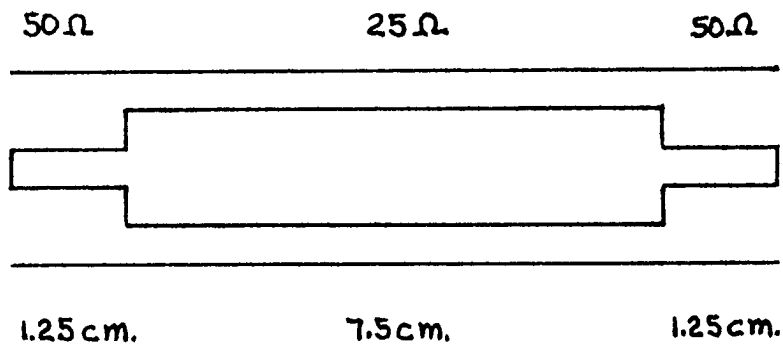
At this point the "Bottoms-Up" performance analysis has been completed, and a look will be taken at the "Tops-Down" process of performance characterization. As has been already identified, the verification process involves the measurement of an independent set of precision devices. Therefore, the verification specifications must include the combined errors of the device measurement process and the verification standards measurement.

In order to support the verification process at user locations, a set of devices has been made available with factory generated data and uncertainty calculations. The uncertainty limits include a worst-case combination of the calibration standard uncertainties, the calibration process, the measurement process, and the verification standard uncertainties.

M only LINEAR
REF 0.0 Units
100.0 mUnits/

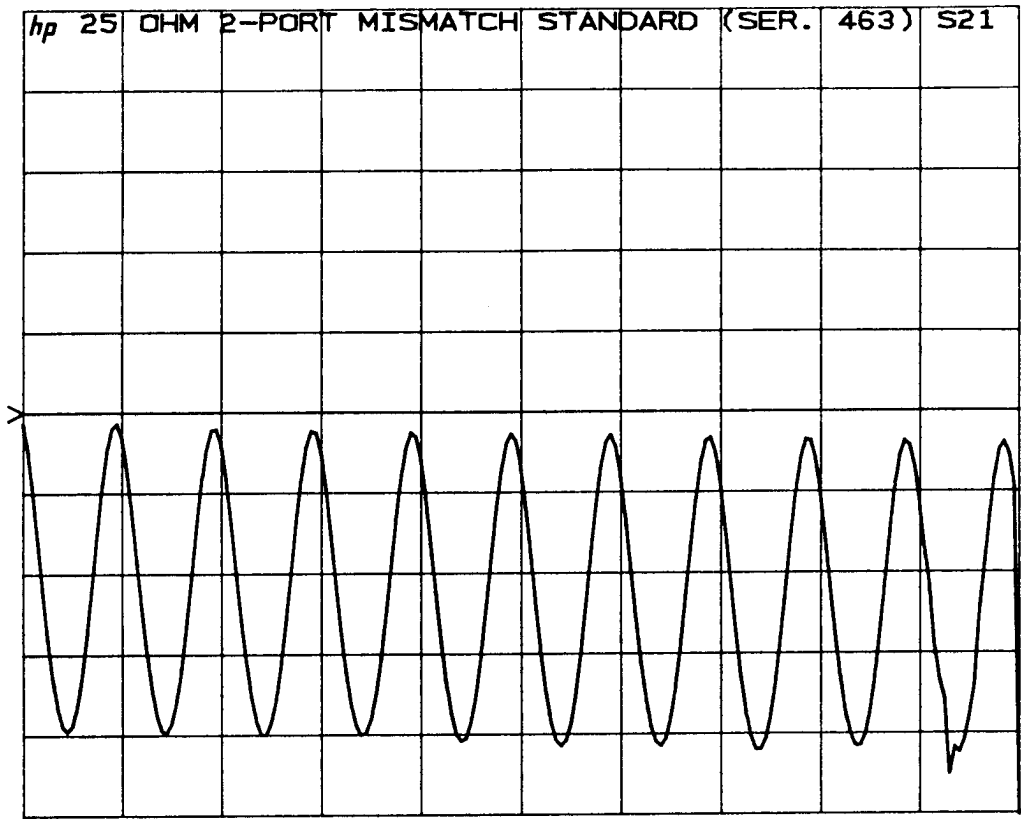


START 0.10000000 GHz
STOP 20.10000000 GHz



25 Ohm 2-Port Impedance Standard - S11 Magnitude Plot

M only log MAG
REF 0.0 dB
 0.5 dB/



START 0.10000000 GHz
STOP 20.10000000 GHz

25 Ohm 2-Port Impedance Standard - S21 Magnitude Plot

25 Ohm 2-Port Mismatch Standard

HEWLETT PACKARD
 VERIFICATION KIT DATA FOR: 8512
 1250-1882 Ser.No.: 463 24 Apr 1984
 8510A System # : 32 by Technician: 904
 PORT IDENTIFICATION : With the device label facing the user;
 Port 1 (A) is on the left and Port 2 (B) is on the right

FREQ GHz	MAG db	S21 UNC +/-	ANG deg	S21 UNC +/-	MAG db	S12 UNC +/-	ANG deg	S12 UNC +/-
.1	.07	.12	-14.2	.85	.07	.12	-14.2	.85
.5	1.11	.25	-66.7	1.74	1.11	.25	-66.7	1.74
1.0	1.98	.30	-120.5	2.12	1.98	.30	-120.5	2.12
2.0	.06	.09	118.4	.84	.07	.09	118.4	.84
3.0	1.99	.30	-1.2	2.34	1.99	.30	-1.1	2.34
4.0	.10	.10	-123.1	1.11	.10	.10	-123.1	1.11
5.0	2.00	.30	118.2	2.55	2.00	.30	118.2	2.55
6.0	.12	.10	-4.6	1.39	.12	.10	-4.5	1.39
7.0	1.99	.30	-122.6	2.77	1.99	.30	-122.5	2.77
8.0	.15	.15	114.0	1.91	.15	.15	114.1	1.91
9.0	2.03	.34	-3.4	3.26	2.03	.34	-3.3	3.26
10.0	.18	.16	-127.4	2.19	.18	.16	-127.3	2.19
11.0	2.04	.34	116.0	3.48	2.04	.34	116.1	3.48
12.0	.22	.17	-8.8	2.46	.22	.17	-8.6	2.46
13.0	2.02	.34	-124.6	3.70	2.03	.34	-124.5	3.70
14.0	.26	.18	109.8	2.73	.26	.18	110.0	2.73
15.0	2.03	.34	-5.1	3.92	2.04	.34	-4.9	3.92
16.0	.30	.19	-131.5	3.01	.30	.19	-131.3	3.01
17.0	2.00	.34	113.8	4.13	2.01	.34	114.0	4.13
18.0	.34	.19	-12.9	3.28	.35	.19	-12.8	3.28

FREQ GHz	MAG lin	S11 UNC +/-	ANG deg	S11 UNC +/-	MAG lin	S22 UNC +/-	ANG deg	S22 UNC +/-
.1	.1170	.0297	-103.8	14.6	.1169	.0297	-103.9	14.6
.5	.4696	.0364	-156.5	4.5	.4697	.0364	-156.6	4.5
1.0	.5976	.0386	149.6	3.8	.5976	.0386	149.4	3.8
2.0	.0250	.0275	-162.2	66.9	.0249	.0275	-159.0	67.2
3.0	.5950	.0384	88.5	3.8	.5949	.0384	88.3	3.8
4.0	.0472	.0279	142.6	34.4	.0475	.0279	142.5	34.2
5.0	.5928	.0383	27.8	3.8	.5934	.0383	27.6	3.8
6.0	.0694	.0283	79.9	23.6	.0694	.0283	79.1	23.6
7.0	.5940	.0384	-33.2	3.8	.5939	.0384	-33.4	3.8
8.0	.0830	.0292	19.9	20.4	.0836	.0292	19.6	20.2
9.0	.5903	.0391	-94.2	3.9	.5910	.0392	-94.4	3.9
10.0	.1085	.0296	-39.8	15.8	.1083	.0296	-39.5	15.9
11.0	.5938	.0392	-155.1	3.9	.5933	.0392	-155.4	3.9
12.0	.1285	.0300	-104.4	13.6	.1287	.0300	-103.8	13.5
13.0	.5934	.0393	143.9	4.0	.5935	.0393	143.5	4.0
14.0	.1501	.0303	-164.4	11.8	.1497	.0303	-164.0	11.8
15.0	.5912	.0391	83.5	4.0	.5914	.0392	82.8	4.0
16.0	.1773	.0309	133.4	10.2	.1768	.0309	133.4	10.2
17.0	.5898	.0392	23.1	4.0	.5900	.0392	22.3	4.0
18.0	.1951	.0312	72.9	9.4	.1958	.0312	72.3	9.4

25 Ohm 2-Port Impedance Standard - Performance Verification Data

50 Ohm 10 cm. Airline

HEWLETT PACKARD
VERIFICATION KIT DATA FOR: 8512

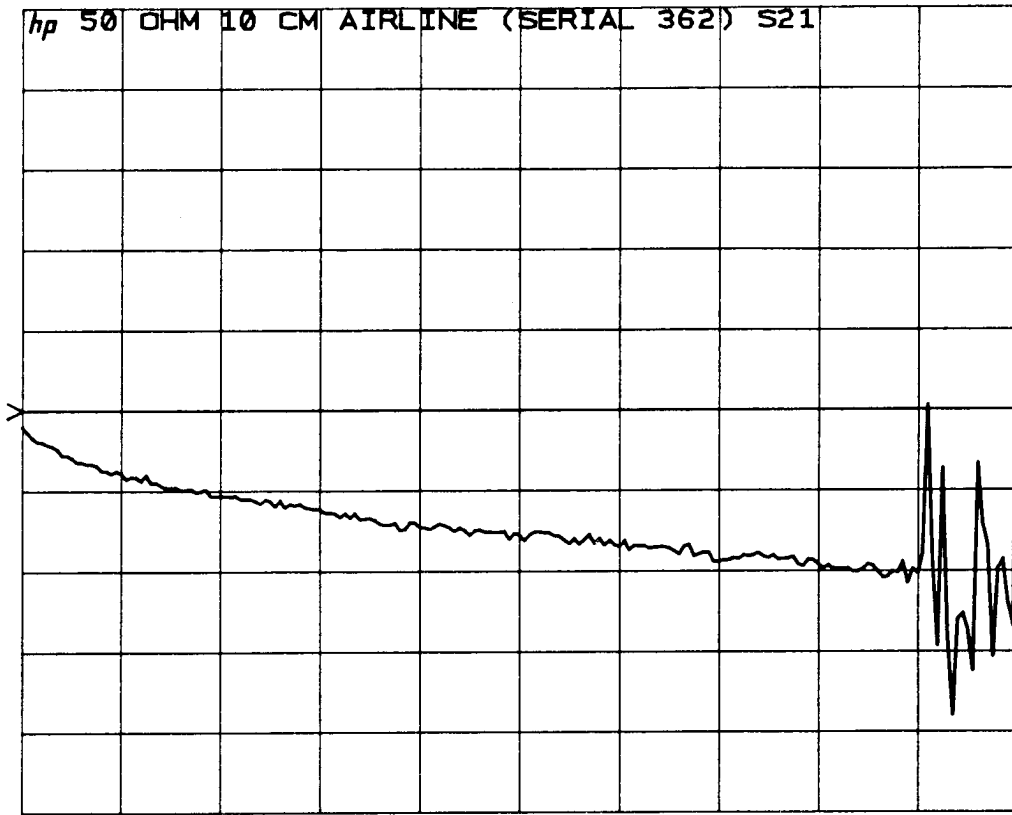
1250-1880 Ser.No.: 362 24 Apr 1984
8510A System # : 32 by Technician: 904
PORT IDENTIFICATION : With the device label facing the user;
Port 1 (A) is on the left and Port 2 (B) is on the right

FREQ GHz	MAG db	UNC +/-	ANG deg	UNC +/-	MAG db	UNC +/-	ANG deg	UNC +/-
.1	.01	.08	-12.0	.58	.01	.08	-12.0	.58
.5	.02	.08	-60.1	.62	.02	.08	-60.1	.62
1.0	.03	.08	-120.1	.68	.03	.08	-120.1	.68
2.0	.04	.08	119.7	.78	.04	.08	119.8	.78
3.0	.05	.08	-.3	.90	.05	.08	-.3	.90
4.0	.05	.08	-120.4	1.01	.05	.08	-120.4	1.01
5.0	.06	.08	119.5	1.12	.06	.08	119.5	1.12
6.0	.06	.08	-.6	1.23	.06	.08	-.6	1.23
7.0	.07	.08	-120.7	1.34	.07	.08	-120.6	1.34
8.0	.07	.12	119.2	1.72	.07	.12	119.3	1.72
9.0	.07	.12	-.9	1.82	.08	.12	-.8	1.82
10.0	.08	.12	-120.9	1.94	.08	.12	-120.8	1.94
11.0	.08	.12	119.0	2.04	.08	.12	119.1	2.04
12.0	.08	.12	-1.1	2.15	.09	.12	-1.0	2.15
13.0	.09	.12	-121.1	2.26	.09	.12	-121.0	2.26
14.0	.09	.12	118.8	2.38	.10	.12	118.9	2.38
15.0	.09	.12	-1.2	2.48	.09	.12	-1.1	2.48
16.0	.09	.12	-121.3	2.60	.10	.12	-121.2	2.60
17.0	.10	.12	118.6	2.71	.10	.12	118.7	2.71
18.0	.10	.12	-1.4	2.81	.10	.12	-1.3	2.81

FREQ GHz	MAG lin	UNC +/-	ANG deg	UNC +/-	MAG lin	UNC +/-	ANG deg	UNC +/-
.1	.0014	.0272	15.8	0.0	.0014	.0272	18.8	0.0
.5	.0030	.0272	-41.3	0.0	.0031	.0272	-42.2	0.0
1.0	.0021	.0272	-140.4	0.0	.0022	.0272	-141.2	0.0
2.0	.0003	.0271	124.5	0.0	.0005	.0271	117.9	0.0
3.0	.0010	.0271	-81.7	0.0	.0011	.0271	-69.5	0.0
4.0	.0013	.0270	-135.1	0.0	.0014	.0270	-135.3	0.0
5.0	.0015	.0270	-149.6	0.0	.0014	.0270	-141.5	0.0
6.0	.0013	.0270	41.2	0.0	.0011	.0270	48.0	0.0
7.0	.0014	.0270	162.6	0.0	.0016	.0270	176.9	0.0
8.0	.0027	.0277	-160.4	0.0	.0028	.0277	-161.6	0.0
9.0	.0006	.0276	101.1	0.0	.0008	.0276	130.3	0.0
10.0	.0033	.0277	63.4	0.0	.0031	.0277	62.9	0.0
11.0	.0012	.0276	117.7	0.0	.0017	.0276	116.9	0.0
12.0	.0005	.0276	-152.8	0.0	.0008	.0276	-166.0	0.0
13.0	.0004	.0276	66.5	0.0	.0007	.0276	70.4	0.0
14.0	.0024	.0276	-26.1	0.0	.0021	.0276	-24.9	0.0
15.0	.0011	.0276	41.8	0.0	.0012	.0276	28.5	0.0
16.0	.0032	.0276	135.0	0.0	.0033	.0276	130.5	0.0
17.0	.0036	.0276	117.8	0.0	.0038	.0276	118.8	0.0
18.0	.0016	.0275	55.2	0.0	.0018	.0275	53.4	0.0

50 Ohm 10 cm. Airline Standard - Performance Verification Data

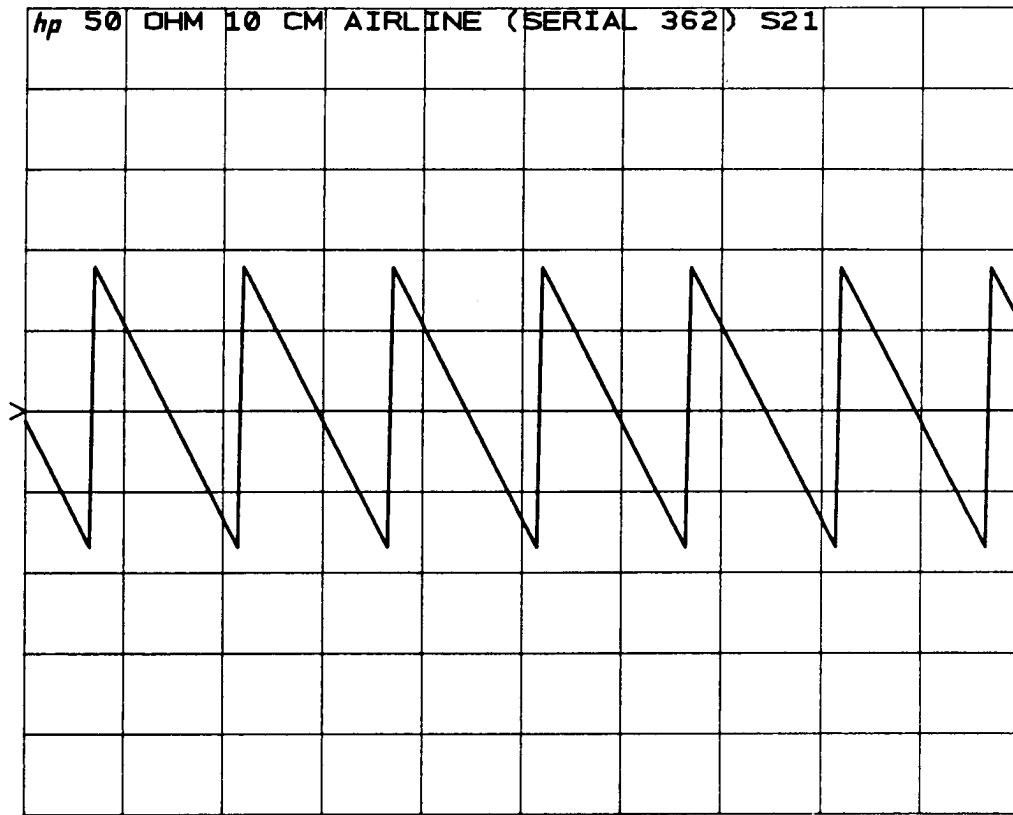
M only log MAG
REF 0.0 dB
0.05 dB/



START 0.10000000 GHz
STOP 20.10000000 GHz

50 Ohm 10 cm. Airline Standard - S21 Magnitude Plot

M only <
REF 0.0 °
100.0 °/



START 0.10000000 GHz
STOP 20.10000000 GHz

50 Ohm 10 cm. Airline Standard - S21 Phase Plot

Note the linear phase response of the 50 Ohm line. This data was generated on a synthesizer-based factory system. Since the transmission line is a uniform precision device, it may be used to compare measurement data at known frequencies or as a frequency discriminator for a swept source when the network analyzer is known to be operating within specification.

HEWLETT PACKARD
 VERIFICATION KIT DATA FOR: 8512 24 Apr 1984

20 dB Pad Ser.No.: 12617
 85051-60001 by Technician: 904

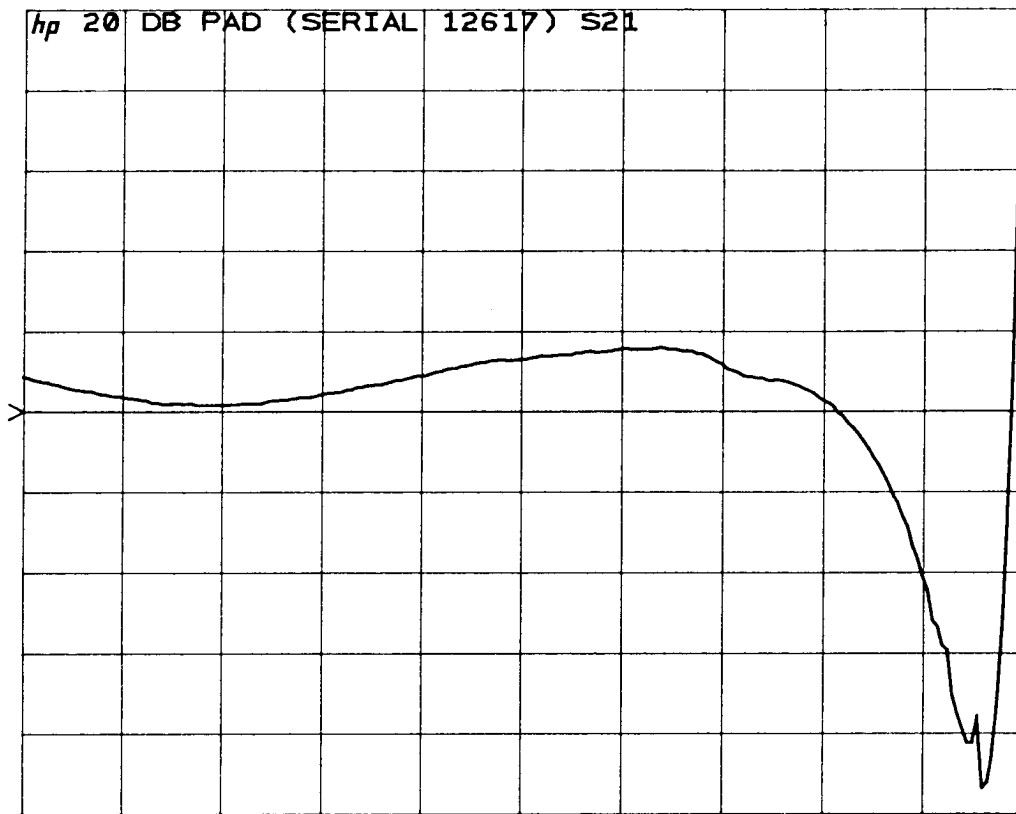
8510A System # : 32
 PORT IDENTIFICATION : With the device label facing the user;
 Port 1 (A) is on the left and Port 2 (B) is on the right

FREQ GHz	MAG db	UNC +/-	ANG deg	S21	UNC +/-	MAG db	UNC +/-	ANG deg	S12	UNC +/-
.1	19.89	.13	-8.6	.92	19.89	.13	-8.5	.92	.92	.13
.5	19.91	.13	-42.8	.97	19.91	.13	-42.8	.97	.97	.13
1.0	19.93	.13	-85.5	1.03	19.93	.13	-85.5	1.03	1.03	.13
2.0	19.96	.14	-170.9	1.16	19.95	.14	-170.9	1.16	1.16	.14
3.0	19.98	.14	103.8	1.28	19.98	.14	103.8	1.28	1.28	.14
4.0	19.98	.14	18.4	1.40	19.98	.14	18.4	1.40	1.40	.14
5.0	19.97	.14	-67.1	1.53	19.97	.14	-67.0	1.53	1.53	.14
6.0	19.95	.14	-152.7	1.65	19.95	.14	-152.6	1.65	1.65	.14
7.0	19.92	.15	121.4	1.77	19.92	.15	121.5	1.77	1.77	.15
8.0	19.89	.18	35.3	2.09	19.89	.18	35.4	2.09	2.09	.18
9.0	19.86	.18	-51.1	2.20	19.86	.18	-51.0	2.20	2.20	.18
10.0	19.84	.18	-137.8	2.31	19.84	.18	-137.7	2.31	2.31	.18
11.0	19.82	.18	135.2	2.41	19.82	.18	135.3	2.41	2.41	.18
12.0	19.81	.17	47.9	2.49	19.81	.17	47.9	2.49	2.49	.17
13.0	19.80	.17	-40.0	2.58	19.80	.17	-39.9	2.58	2.58	.17
14.0	19.85	.17	-128.3	2.69	19.85	.17	-128.3	2.69	2.69	.17
15.0	19.90	.17	143.4	2.81	19.91	.17	143.5	2.81	2.81	.17
16.0	19.96	.18	54.4	2.95	19.96	.18	54.4	2.95	2.95	.18
17.0	20.11	.18	-35.0	3.10	20.12	.18	-34.9	3.10	3.10	.18
18.0	20.46	.18	-123.8	3.22	20.46	.18	-123.8	3.22	3.22	.18

FREQ GHz	MAG lin	UNC +/-	ANG deg	S11	UNC +/-	MAG lin	UNC +/-	ANG deg	S22	UNC +/-
.1	.0021	.0073	10.1	0.0	.0184	.0076	168.7	24.0	24.0	.0076
.5	.0040	.0073	17.3	129.8	.0189	.0076	124.5	23.3	23.3	.0076
1.0	.0064	.0074	-5.3	69.8	.0213	.0077	74.3	20.9	20.9	.0077
2.0	.0117	.0075	-62.9	37.3	.0289	.0079	-15.1	15.7	15.7	.0079
3.0	.0159	.0076	-134.9	27.6	.0356	.0080	-98.0	13.0	13.0	.0080
4.0	.0197	.0077	148.7	22.4	.0421	.0082	-178.9	11.2	11.2	.0082
5.0	.0248	.0078	73.9	18.1	.0497	.0084	103.4	9.7	9.7	.0084
6.0	.0301	.0079	.8	15.2	.0557	.0085	28.2	8.9	8.9	.0085
7.0	.0345	.0080	-71.5	13.4	.0582	.0086	-47.4	8.5	8.5	.0086
8.0	.0379	.0086	-143.4	13.1	.0579	.0091	-126.3	9.1	9.1	.0091
9.0	.0398	.0086	144.5	12.6	.0549	.0090	153.8	9.5	9.5	.0090
10.0	.0397	.0086	72.6	12.6	.0510	.0089	76.6	10.2	10.2	.0089
11.0	.0370	.0086	2.1	13.4	.0439	.0087	1.1	11.6	11.6	.0087
12.0	.0313	.0084	-67.2	15.6	.0319	.0085	-79.3	15.4	15.4	.0085
13.0	.0226	.0083	-135.8	21.3	.0205	.0082	176.9	23.3	23.3	.0082
14.0	.0130	.0080	156.9	36.3	.0259	.0083	55.5	18.6	18.6	.0083
15.0	.0076	.0079	41.3	62.7	.0446	.0087	-33.7	11.4	11.4	.0087
16.0	.0129	.0080	-90.9	36.4	.0604	.0091	-111.2	8.9	8.9	.0091
17.0	.0174	.0081	-171.0	27.2	.0696	.0093	175.6	7.9	7.9	.0093
18.0	.0147	.0080	103.1	32.0	.0708	.0093	100.3	7.8	7.8	.0093

20 dB Pad - Performance Verification Data

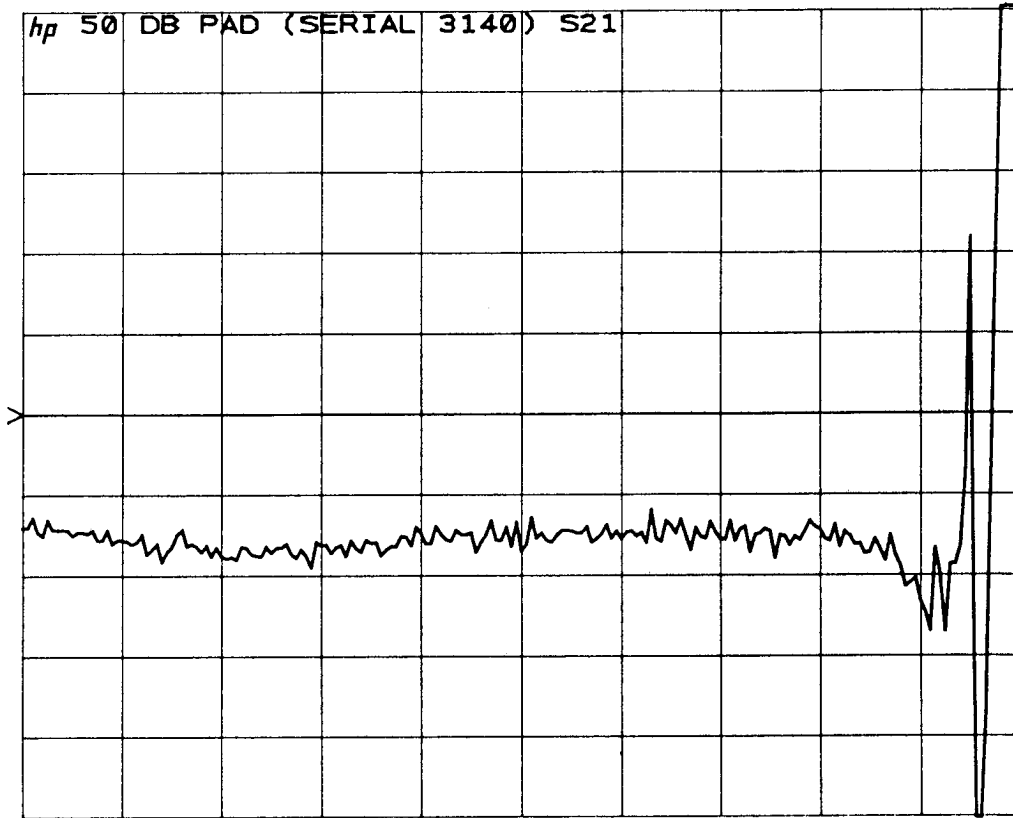
M only log MAG
REF -20.0 dB
0.25 dB/



START 0.100000000 GHz
STOP 20.100000000 GHz

20 dB Pad - S21 Magnitude Plot

M only log MAG
REF -50.0 dB
0.5 dB/



START 0.100000000 GHz
STOP 20.100000000 GHz

50 dB Pad - Performance Verification Data

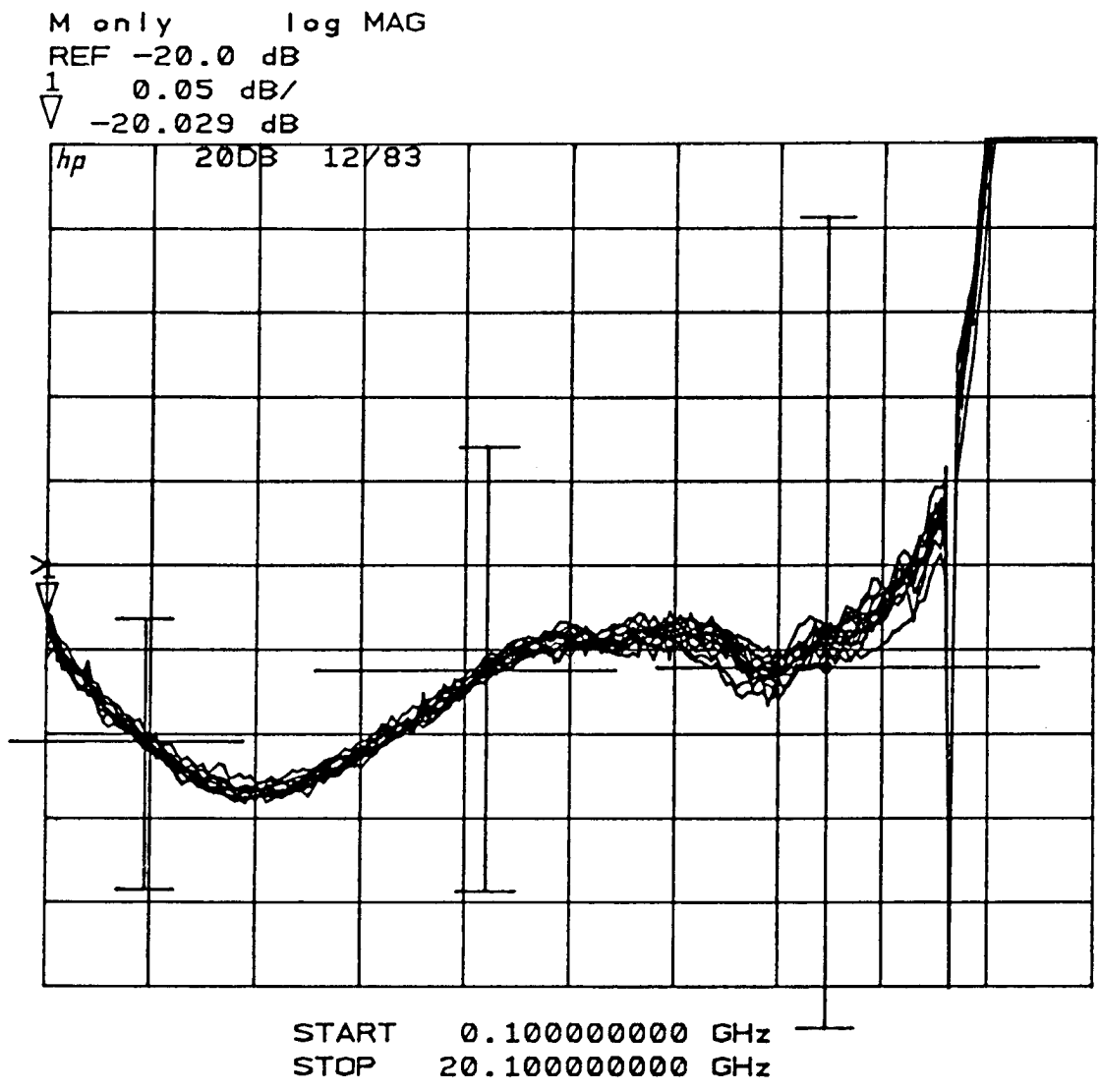
HEWLETT PACKARD
 VERIFICATION KIT DATA FOR: 8512

50 dB Pad
 85051-60002 Ser.No.: 3140 24 Apr 1984
 8510A System # : 32 by Technician: 904
 PORT IDENTIFICATION : With the device label facing the user;
 Port 1 (A) is on the left and Port 2 (B) is on the right

FREQ GHz	MAG db	UNC +/-	ANG deg	S21	UNC +/-	MAG db	UNC +/-	ANG deg	S12	UNC +/-
.1	50.70	.86	-8.1	5.47	50.70	.86	-8.2	5.47		
.5	50.76	.87	-39.2	5.54	50.75	.87	-39.3	5.54		
1.0	50.72	.86	-79.3	5.58	50.74	.87	-79.3	5.59		
2.0	50.78	.87	-157.3	5.72	50.81	.87	-157.1	5.74		
3.0	50.85	.88	123.6	5.87	50.86	.88	123.7	5.87		
4.0	50.83	.87	46.1	5.97	50.83	.87	46.1	5.97		
5.0	50.82	.87	-32.6	6.08	50.85	.88	-32.5	6.10		
6.0	50.79	.87	-110.0	6.18	50.78	.87	-110.1	6.18		
7.0	50.78	.87	170.8	6.29	50.82	.88	170.7	6.32		
8.0	50.70	1.12	92.6	7.88	50.72	1.13	92.4	7.90		
9.0	50.75	1.13	14.0	8.03	50.68	1.12	13.7	7.98		
10.0	50.66	1.12	-65.0	8.09	50.71	1.13	-64.9	8.12		
11.0	50.72	1.13	-143.6	8.25	50.72	1.13	-143.9	8.25		
12.0	50.72	1.13	137.0	8.37	50.74	1.13	137.1	8.38		
13.0	50.66	1.13	58.5	8.45	50.71	1.13	58.5	8.48		
14.0	50.73	1.14	-20.7	8.61	50.73	1.14	-20.9	8.61		
15.0	50.71	1.13	-99.5	8.71	50.72	1.14	-99.9	8.72		
16.0	50.70	1.13	-179.1	8.82	50.74	1.14	-179.6	8.85		
17.0	50.87	1.16	99.8	9.05	50.81	1.15	99.4	9.01		
18.0	51.02	1.17	13.1	9.26	50.99	1.17	12.6	9.23		

FREQ GHz	MAG lin	UNC +/-	ANG deg	S11	UNC +/-	MAG lin	UNC +/-	ANG deg	S22	UNC +/-
.1	.0088	.0072	171.7	48.3	.0196	.0075	172.9	21.9		
.5	.0089	.0072	133.8	48.1	.0195	.0074	143.7	22.1		
1.0	.0094	.0072	90.6	45.4	.0198	.0075	109.3	21.7		
2.0	.0123	.0073	7.5	34.6	.0212	.0075	39.4	20.4		
3.0	.0147	.0074	-69.7	29.2	.0208	.0075	-28.8	20.8		
4.0	.0166	.0074	-145.0	25.8	.0196	.0075	-100.0	21.9		
5.0	.0195	.0074	140.2	22.1	.0206	.0075	-175.4	21.0		
6.0	.0229	.0075	67.5	19.0	.0233	.0075	114.5	18.7		
7.0	.0263	.0076	-2.5	16.7	.0254	.0076	50.2	17.3		
8.0	.0302	.0082	-71.3	15.8	.0260	.0081	-14.9	18.1		
9.0	.0341	.0083	-138.5	14.1	.0262	.0081	-85.0	17.9		
10.0	.0378	.0084	155.7	12.9	.0293	.0082	-156.7	16.2		
11.0	.0409	.0085	90.7	12.0	.0353	.0083	137.5	13.7		
12.0	.0433	.0085	25.6	11.4	.0406	.0084	75.8	12.1		
13.0	.0459	.0086	-39.7	10.9	.0430	.0085	14.8	11.5		
14.0	.0491	.0086	-103.4	10.3	.0449	.0085	-50.1	11.1		
15.0	.0513	.0087	-164.5	9.9	.0495	.0087	-116.4	10.2		
16.0	.0515	.0087	136.8	9.9	.0571	.0088	-177.3	9.1		
17.0	.0496	.0087	77.5	10.2	.0626	.0090	126.0	8.4		
18.0	.0496	.0087	9.7	10.2	.0559	.0088	73.3	9.3		

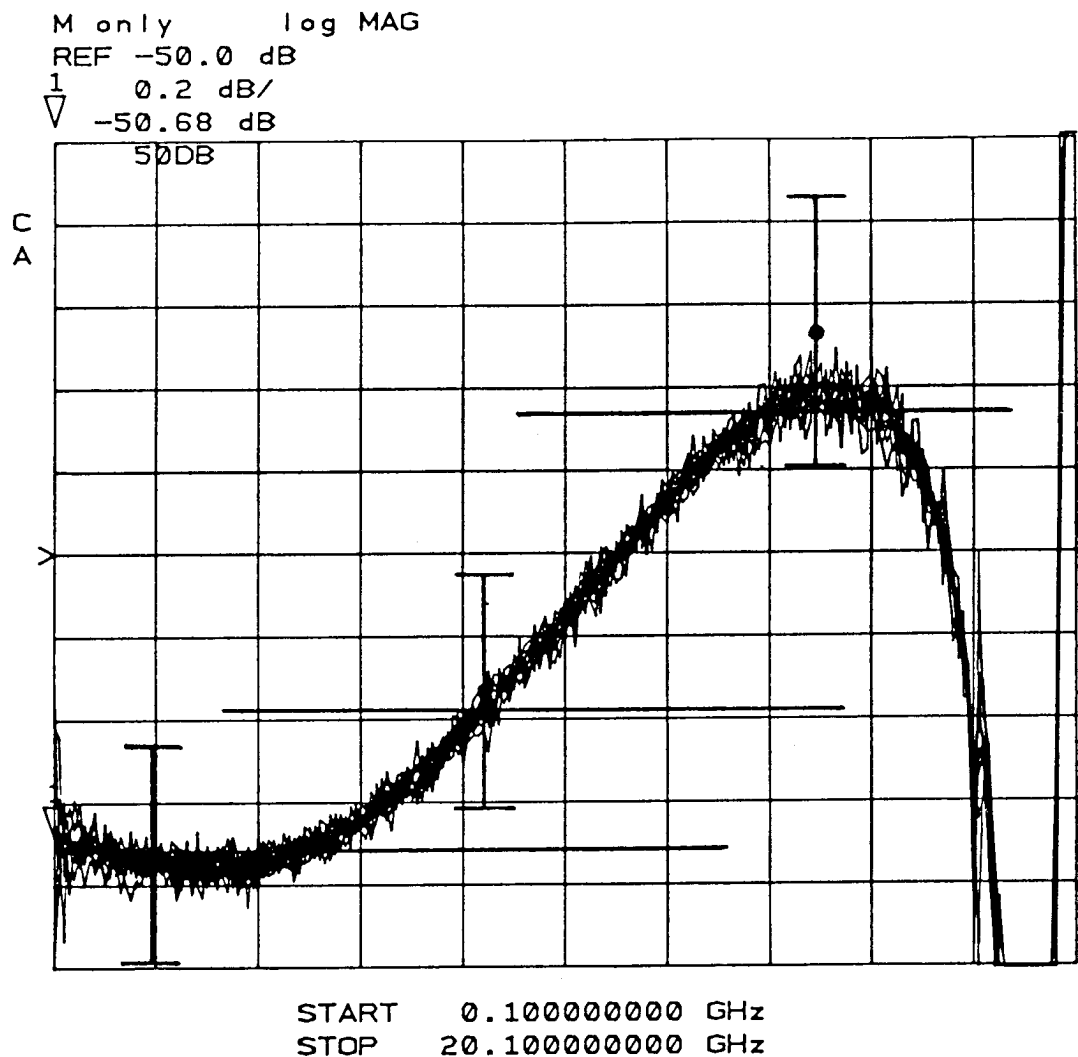
50 dB Pad - S21 Magnitude Plot



20 dB Pad Plot - NBS Data Points - 7 8510 Systems - S21 and S12

As a means of validating the "Bottoms-Up" specification method, a cross check experiment was performed with some devices which had a long history of measurement at the National Bureau of Standards.

This multiple plot shows S21 and S12 magnitude measurements of a 20 dB fixed attenuator made on three 8510A/8512A systems and four 8510A/8514A systems (14 plots). This same attenuator has also been measured at NBS in 1975, 1978, 1980, and 1982. The 1982 NBS measurement uncertainty limits at 2.0, 8.5, and 15.0 GHz are shown by the capped vertical lines, while the actual measurements are shown by dots. The intercepts of the horizontal lines with the vertical uncertainty limits locate the mean value of the NBS measurements over the four years; note the close agreement with the 8510 data (.05 dB/division).



50 dB Pad Plot - NBS Data Points - 7 8510 Systems - S21 and S12

This multiple plot shows S21 and S12 magnitude measurements of a 50 dB fixed attenuator made on three 8510A/8512A systems and four 8510A/8514A systems (14 plots). This same attenuator has also been measured at NBS in 1975, 1978, 1980, and 1982. The 1982 NBS measurement uncertainty limits at 2.0, 8.5, and 15.0 GHz are shown by the capped vertical lines, while the actual measurements are shown by dots. The intercepts of the horizontal lines with the vertical uncertainty limits locate the mean value of the NBS measurements over the four years; note the close agreement with the 8510 data (.20 dB/division).

SPECIFICATION METHOD SUMMARY

BOTTOMS-UP METHOD

MOST PRECISE METHOD FOR DETERMINING MEASUREMENT ACCURACY

INDEPENDENT VERIFICATION OF SPECIFICATIONS IS NOT PRACTICAL UNLESS THE VERIFICATION STANDARDS ARE SIGNIFICANTLY SUPERIOR TO THE CALIBRATION STANDARDS; AN UNLIKELY CIRCUMSTANCE

TOPS-DOWN METHOD

PROVIDES A CONVENIENT WAY TO CROSS-CHECK PERFORMANCE OF THE SYSTEM AND CALIBRATION TO AN INDEPENDENT SET OF VERIFICATION STANDARDS

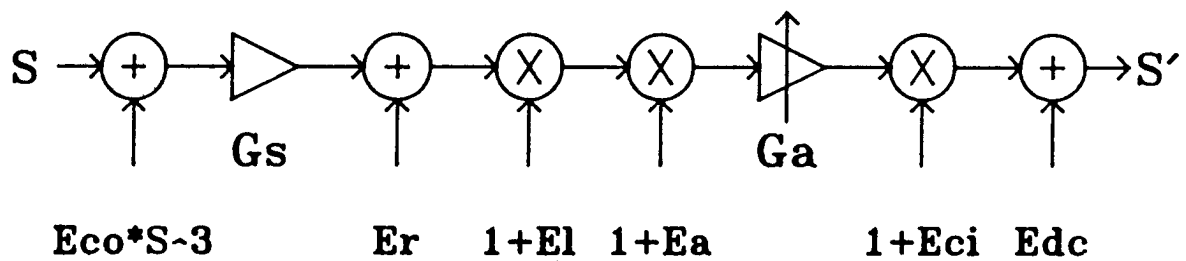
PROVIDES A DEGREE OF COMFORT BY MEASURING FAMILIAR, WELL-KNOWN VERIFICATION STANDARDS

LIMITED IN ACCURACY TO THE COMBINED UNCERTAINTIES OF THE CALIBRATION STANDARDS, CALIBRATION PROCESS, MEASUREMENT PROCESS, AND VERIFICATION STANDARDS

PROVIDES INSIGHT ONLY AT SELECTED PARAMETER VALUES (DETERMINED BY THE CHOICE OF VERIFICATION DEVICES)

APPENDIX I - 8510 Dynamic Accuracy Model

The following model is used to construct the dynamic accuracy curves for the various configurations of the 8510 system. These curves are plotted in Section 1-1 of the 8510 Operating and Service Manual.



E_a = I.F. autorange gain error

E_{co} = compression error

E_{ci} = circularity Error

E_{dc} = effective D.C. offset error

E_l = I.F. linearity error

E_r = I.F. residual signal error

G_a = I.F. autorange gain

G_s = sampler gain

where all the terms are expressed in linear format.

Definition of Dynamic Accuracy Error Terms

E_a = I.F. autorange gain error

The autorange gain error is a discontinuity formed in the detected level as the autorange control changes gain level. These errors are less than $\pm .005$ dB for the 12 and 24 dB stages and $\pm .01$ dB for the 36 and 48 dB stages.

E_c = Compression error

Compression errors are caused primarily by the samplers. Since compression is always small, a third order model has been used for analysis. Compression is the only error which is assumed to be correlated between calibration and measurement. This is because the direction of the compression is always predictable; it always makes the detected signal appear lower in amplitude. The maximum input level at which .1 dB compression occurs is specified (-10 dBm).

E_{ci} = Circularity error

The circularity errors are caused by the synchronous detectors. In principle, they result from a lack of perfect quadrature between the two axes of the detectors and from slight differences in the axis gains. These errors are manifested as a change in magnitude as a function of phase change at constant input amplitude. These effects are less than $\pm .003$ dB. Basic phase linearity is less than $\pm .001$ degrees/degree, not to exceed .02 degrees when measured at the reference signal level.

E_{dc} = Effective D.C. offset error

The effective D.C. offset is the residual offset after I.F. correction. Its contribution is comparable to an I.F. input level of -100 dBm.

E_l = I.F. linearity

This term is caused predominantly by localized non-linearities in the 20 MHz I.F. system at levels below the traditional high-level compression zone. Both simple non-linearities and hysteresis effects are experienced. Overall performance is within $\pm .003$ dB.

E_r = I.F. residuals

This error is caused by leakage from the I.F. local oscillators into the signal path. The residuals are measured by terminating the I.F. input port, heavily averaging the noise, and reading the remaining signal level. Performance is guaranteed to be better than -120 dBm,

Definition of Dynamic Accuracy Gain Terms

Ga = I.F. autorange gain

The autorange circuit has five gain positions 0, 12, 24, 36, and 48 dB. The gain value is important to the overall error model, since it affects the contribution of the D.C. offset.

Gs = Gain of the sampler

The gain (conversion efficiency) of the sampler exhibits a frequency dependent characteristic which affects signal amplitudes in the I.F. system. As a result, the relative contribution of selected error sources is somewhat frequency dependent; these effects may be seen in the plots of dynamic accuracy and S-parameter uncertainty limits.

From the flow graph model, the following equation for s' can be derived:

$$s' = ((s - E_{co} \cdot s^3) \cdot G_s + E_r)(1 + E_l)(1 + E_a) \cdot G_a \cdot (1 + E_{ci}) + E_{dc}$$

Since the 8510 software divides the output of the I.F. by the autorange gain, we can rewrite the equation as:

$$s' = ((s + E_{co} \cdot s^3) \cdot G_s + E_r)(1 + E_l)(1 + E_a)(1 + E_{ci}) + E_{dc} / G_a$$

However, two measurements are always made; one is the measurement made at the calibration level and the other is the measurement of the device under test ($s = c$ and $s = m$, respectively). The m data is normalized by the c data, so the desired output is m/c . However, the actual output is m'/c' or:

$$\frac{m'}{c'} = \frac{((m - E_{co} \cdot m^3) \cdot G_s - E_r)(1 - E_l)(1 - E_{am})(1 - E_{ci}) - E_{dc} / G_{am}}{((c - E_{co} \cdot c^3) \cdot G_s + E_r)(1 + E_l)(1 + E_{ac})(1 + E_{ci}) + E_{dc} / G_{ac}}$$

where G_{am} is autorange gain for measurement
 E_{am} is autorange error for measurement
 G_{ac} is autorange gain for calibration
 E_{ac} is autorange error for calibration

In the expressions above, subscripts were added to E_a and G_a because their values change depending on the input signal level (i.e. the setting of the autorange gain). The other error coefficients are constant independent of signal level. Also, since all of the error terms, except compression, have random phase, the signs of the error terms can be either + or -. Using - in the numerator and + in the denominator yields a worst case error in the negative direction.

Compression, however, does not have random phase; it only makes the input appear smaller than it actually is. Therefore, the signs of the compression terms are equal. Also, as explained above, the signs of the errors were chosen for the worst case error in the negative direction. When m is larger than c , the compression error is negative. However, when m is smaller than c , the compression error is positive. Therefore, the sign of E_{co} must change when m is less than c . The following equation expresses the compression error as \pm to account for this change in sign.

$$\frac{m'}{c'} = \frac{((m \pm E_{co} \cdot m^3) \cdot G_s - E_r)(1 - E_l)(1 - E_{am})(1 - E_{ci}) - E_{dc} / G_{am}}{((c \pm E_{co} \cdot c^3) \cdot G_s + E_r)(1 + E_l)(1 + E_{ac})(1 + E_{ci}) + E_{dc} / G_{ac}}$$

Therefore, the error, which is the difference between the desired (m/c) and the actual is:

$$E_{if} = \frac{m}{c} - \frac{((m \pm E_{co} \cdot m^3) \cdot G_s - E_r)(1 - E_l)(1 - E_{am})(1 - E_{ci}) - E_{dc} / G_{am}}{((c \pm E_{co} \cdot c^3) \cdot G_s + E_r)(1 + E_l)(1 + E_{ac})(1 + E_{ci}) + E_{dc} / G_{ac}}$$

In the program which generated the 8510 dynamic accuracy curves, the autorange gain was assumed equal to 1 (0 dB) for the calibration measurement. The autorange error is defined equal to zero for the I.F. gain equal to 0 dB. Therefore, the equation reduces to:

$$E_{if} = \frac{m}{c} - \frac{((m \pm E_{co} \cdot m^3) \cdot G_s - E_r)(1 - E_l)(1 - E_{am})(1 - E_{ci}) - E_{dc} / G_{am}}{((c \pm E_{co} \cdot c^3) \cdot G_s + E_r)(1 + E_l)(1 + E_{ci}) + E_{dc}}$$

APPENDIX 2 - 8510 / 8512A Performance Specifications

The specification data listed in the following table is based on a statistical performance analysis of a large number of production systems. In almost every case, the specification limit was set three standard deviations from the mean value (in the high-confidence direction if the specification is single-sided). In regular production operation, any parameter which exceeds the specification limit causes the unit to be returned to a prior workstation for adjustment or rework. An analysis of the overall production operation has shown that system-level specifications meet a confidence level of 99.9%.

8510 / 8512 Performance Specifications

	8.0 GHz	18.0 GHz
=====	=====	=====
D = residual directivity	-50.0 dB	-50.0 dB
Ms = residual source match	-40.0 dB	-40.0 dB
Tr = residual reflection tracking	+-.050 dB	+-.050 dB
C = residual crosstalk	-90.0 dB	-90.0 dB
Ml = residual load match	-40.0 dB	-40.0 dB
Tt = residual transmission tracking	+-.015 dB	+-.030 dB
Cs = cable stability (0.1 deg/GHz)	0.8 deg	1.8 deg
Nh = high level noise (rms)	+-.0015 dB	+-.0020 dB
Nl = low level noise (rms)	-93.0 dB	-90.0 dB
Rr1 = port-1 reflection repeatability	-70.0 dB	-65.0 dB
Rt1 = port-1 transmission repeatability	-70.0 dB	-65.0 dB
Rr2 = port-2 reflection repeatability	-70.0 dB	-65.0 dB
Rt2 = port-2 transmission repeatability	-70.0 dB	-65.0 dB
Ea = I.F. autorange gain error (12 dB)	+-.005 dB	+-.005 dB
Ea = I.F. autorange gain error (24 dB)	+-.005 dB	+-.005 dB
Ea = I.F. autorange gain error (36 dB)	+-.010 dB	+-.010 dB
Ea = I.F. autorange gain error (48 dB)	+-.010 dB	+-.010 dB
Eco = compression error; .100 dB at	-10.0 dBm	-10.0 dBm
Eci = circularity error	+-.003 dB	+-.003 dB
Edc = effective D.C. offset error	-100.0 dBm	-100.0 dBm
El = I.F. linearity error	+-.003 dB	+-.003 dB
Er = I.F. residual signal error	-120.0 dBm	-120.0 dBm
Gs = sampler gain	-3.0 dB	-4.0 dB
Incremental Phase Linearity = +- .001 degrees/degree, <.02 deg. total		
R = reference level (typ @ 20 MHz I.F.)	-22.0 dBm	-26.0 dBm

